Meteorol. Atmos. Phys. 49, 43–67 (1992)

Meteorology and Atmospheric Physics

551.515

Department of Marine, Earth, and Atmospheric Sciences, North Carolina State University, Raleigh, U.S.A.

Numerical Modeling Studies of Lee Mesolows, Mesovortices and Mesocyclones with Application to the Formation of Taiwan Mesolows

Y.-L. Lin, N.-H. Lin, and **R. P. Weglarz**

With 16 Figures

Received December 4, 1991
Revised April 10, 1992

Summary

Numerical experiments are performed for inviscid flow past an idealized topography to investigate the formation and development of lee mesolows, mesovortices and mesocyclones. For a nonrotating, low-Froude number flow over a bell-shaped moutain, a pair of mesovortices form on the lee slope, move downstream and weaken at later times. The advection speed of the lee vortices is found to be about two-thirds of the basic wind velocity, which is due to the existence of a reversed pressure gradient just upstream of the vortices. The lee vortices do not concur with the upstream stagnation point in time, but rather form at a later time. It is found that a pair of lee vortices form for a flow with $Fr = 0.66$, but take a longer time to form than in lower-Froude number flows. Since the lee vortices are formed rather progressively, their formation may be explained by the baroclinically-induced vorticity tilting as the mountain waves become more and more nonlinear.

A stationary mesohigh and mesolow pressure couplet forms across the mountain and is produced in both high and low-Froude number flows. The results of the high Froude number simulations agree well with the classical results predicted by linear, hydrostatic mountain wave theory. It is found that the lee mesolow is not necessarily colocated with the lee vortices. The mesolow is formed by the downslope wind associated with the orographically forced gravity waves through adiabatic warming. The earth's rotation acts to strengthen (weaken) the cyclonic (anticyclonic) vortex and shifts the lee mesolow to the right for an observer facing downstream. The cyclonic vortex then develops into a mesocyclone with the addition of planetary vorticity at later times. For a flow over a steeper mountain, the disturbance is stronger even though the Froude number is kept the same.

For a southwesterly flow past the real topography of Taiwan, there is no stagnation point or lee vortices formed because the impinging angle of the flow is small. A major mesoscale low forms to the southeast of the Central Mountain Range (CMR), while a mesohigh forms upstream. For a westerly flow past Taiwan, a stagnation point forms upstream of the mountain and a pair of vortices form on the lee and move downstream at later times. The cyclonic vortex then develops into a mesocyclone. A mesolow also forms to the southeast of Taiwan. For a northeasterly flow past Taiwan, the mesolow forms to the northwest of the mountain. Similar to flows over idealized topographies, the Taiwan mesolow is formed by the downslope wind associated with mountain waves through adiabatic warming. A conceptual model of the Taiwan southeast mesolow and mesocyclone is proposed.

1. Introduction

Shallow mesoscale low pressure centers (mesolows) often form to the southeast or to the northwest of Taiwan when the Mei-Yu front passes over the island (Chen, 1980). Figure 1 shows three examples of the mesolows formed to the southeast or northwest of Taiwan, which were observed at 0600 UTC 12 June 1975 (Chen, 1980), 1200 UTC 13 May 1987 (Wang, 1989), and 1800 UTC 16 May 1987 during TAMEX (Kuo and Chen, 1990). When the east-west or southwest-northeast oriented Mei-Yu front impinges on the Central Mountain Range (CMR), it splits into two branches. The

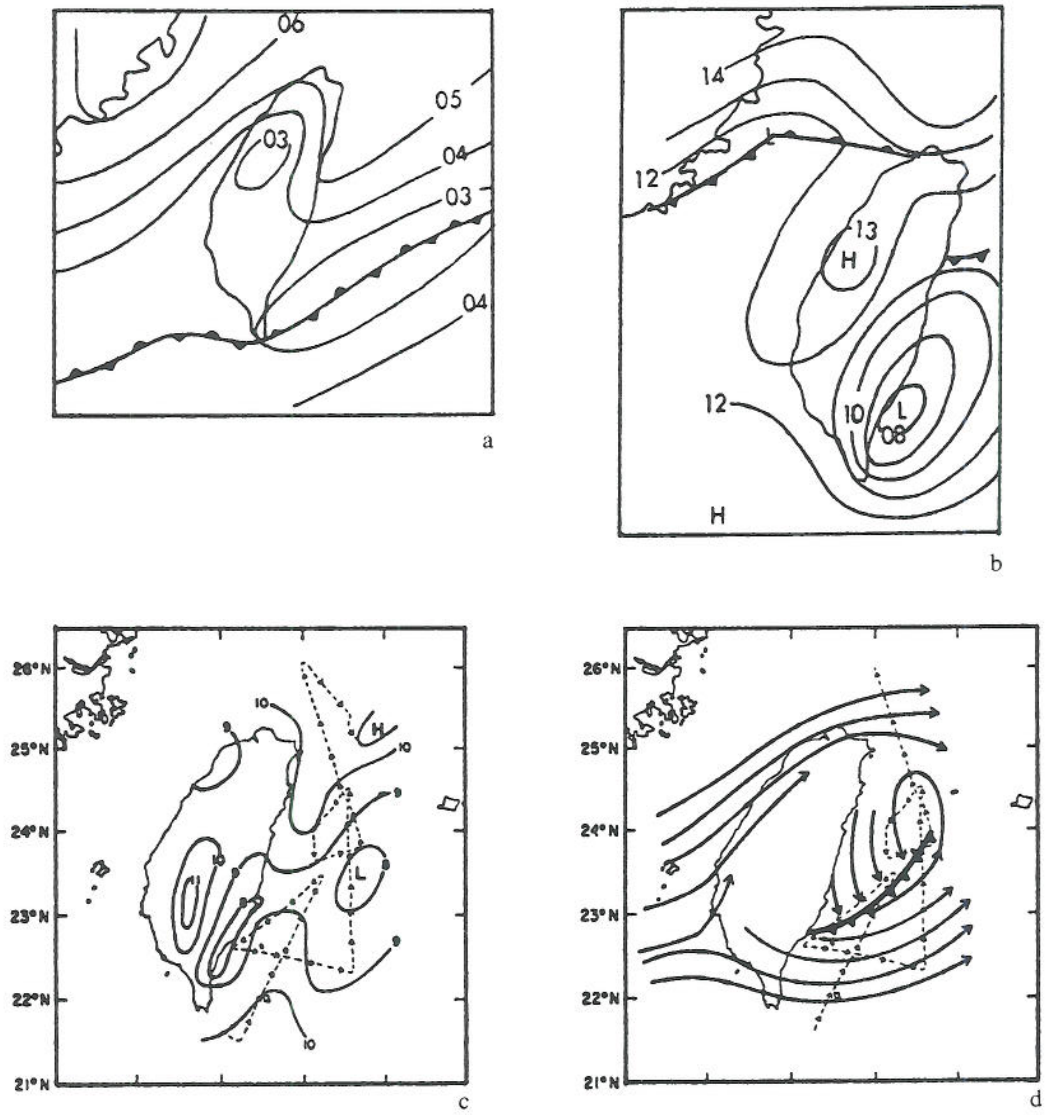

Fig. 1. Examples of mesolows formed to the southeast of Taiwan during the Mei-Yu season: (a) Surface analysis at 0600 UTC, June 12, 1975 (Reproduced from Chen, 1980), (b) Surface analysis at 1200 UTC, May 13, 1987 (Reproduced from Wang, 1989), and (c) Sea-level pressure at 1800 UTC, May 16, 1987 and (d) 900 mb streamlines for (c) (From Kuo and Chen, 1990)

eastern branch moves southward faster than the western branch (Fig. 1b). On the upstream side of the CMR, the southwesterly wind prevails before the frontal passage. Occasionally, the prevailing wind before the frontal passage is westerly (Wang, 1989). The location of the southeast mesolow shifts farther to the south for a westerly flow compared with that for a southwesterly flow (Wang, 1989). The wind speed may vary from 5 to 15 ms^{-1} in the lower layer. The wind turns to a more northeasterly direction behind the Mei-Yu front. The northwest low is responsible for enhancing the local rainfall which often leads to flash floods in northern Taiwan during the Mei-Yu season (May 15–June 15). The southeast low occurs more frequently and more prominantly than the northwest low. The southeast low has less significant impact on the weather in Taiwan because it is located downstream of the prevailing southwesterly or westerly wind. However, it is essential to understand the formation mechanism of the mesolow since it is highly related to the flow structure over and around the CMR of Taiwan. The dynamics governing the formation mechanism will also help in understanding the orographic effects on Mei-Yu fronts and Mesoscale Convective

Systems, which is one of the major scientific objectives of the TAMEX field project (Kuo and Chen, 1990).

The frequency distribution of mesolows in a six year period (1972–1977) during the Mei-Yu season indicates that about 72.5% of the mesolows form to the southeast of Taiwan, while the rest form to the northwest (e.g., Kuo and Chen, 1990). Occasionally, two mesolows may form simultaneously to the east and to the southeast of the island, such as those observed during TAMEX IOP#2 (Fig. 1c). The southeast mesolow often forms near the mountain and elongates in the northeast-southwest direction. A typical southeast mesolow has a short axis of about 50–100 km and a pressure perturbation of 3 to 5 mb. The northwest mesolow forms less frequently and is smaller in size (Fig. 1a). Observations indicate that mesolows do not form at any particular time of the day (Figs. 1a and b). The Taiwan mesolow is shallow and has a height of about 1.5 to 2 km. Observations also show that the southeast mesolow is warmer and less humid than its surroundings, which may suggest that the formation of the low is partially related to the adiabatic warming associated with the downslope wind on the lee side of the CMR. Accompanying the southeast mesolow is a mesoscale high pressure center formed to the west or northwest of Taiwan on the windward slope. The upslope mesohigh is relatively weaker, but pronounced. When the southwesterly flow impinges upon the mountain, the flow splits on the upwind slope and most of the low-level flow is blocked and forced to go around the CMR (Fig. 1d). In order to understand the dynamics of the Taiwan mesolow, a basic study of flow over an idealized topography is needed.

For nonrotating hydrostatic flow over a two-dimensional ridge, a high and low pressure form on the upstream and downstream sides of the mountain, respectively. Observational studies also show that a high-low pressure couplet is often generated for flow over a mesoscale mountain when the Rossby number is approximately equal to 1 (Smith, 1982). Numerical simulations indicate that upstream air parcels tend to deflect to the left due to the mountain-induced high pressure (e.g., Thorsteinsson, 1988). The high-low pressure couplet has been observed when the southeast mesolow forms during the Mei-Yu season (e.g., Wang, 1989; Kuo and Chen, 1990; see Fig. 1). Thus, the formation of the Taiwan mesolow may be associated with the downslope winds through adiabatic warming. In a recent study, Kuo and Chen (1990) suggested that cyclonic vorticity is produced by strong air-column stretching which then induces the mesolow through adiabatic warming and drying. In addition, it is important to note that the vorticity stretching can only contribute to the later development of lee vortices, but cannot contribute to their initial formation, according to the vorticity equation. In this study, we will show that the cyclonic lee mesovortex will develop into a mesocyclone in a rotating flow past both idealized and real mountains.

Traditional observational data analysis (e.g., Wang, 1989) indicates that the southeast Taiwan mesolow is associated with a closed circulation. In this study, we define a mesovortex as a mesoscale region of closed circulation. Thus the formation mechanisms of the Taiwan mesolow may be related to the problem of a three-dimensional flow past an isolated mountain, which has been studied by a number of authors (for a review, see Smith, 1989a). In particular, we are interested in low Froude-number (U/Nh) flow because of the height of the CMR, where U is the basic wind velocity, N the Brunt-Vaisala frequency, and h the mountain height. The CMR runs through Taiwan in a NNE-SSW direction with a width of about 120 km, a length of about 300 km and an average height of 2 km. There exist two major peaks above 3 km with the highest peak occurring at an altitude of roughly 4 km above sea level. The flow response around three-dimensional obstacles with low Froude number has been investigated experimentally (e.g., Hunt and Snyder, 1980) and numerically (e.g., Smolarkiewicz et al., 1988; Smolarkiewicz and Rotunno, 1989a). In recent numerical studies by Smolarkiewicz and Rotunno (1989a, b), it is found that a pair of lee vortices tends to form when an inviscid stratified flow passes a bell-shaped mountain with a Froude number less than 0.5. This pair of lee vortices tend to reach a steady state after a nondimensional time $Ut/a = 3$, where a is the half-width of the mountain. The Froude number associated with the flow varies from 0.055 to 2.2 in their study. Due to the interest in lee vortices, their discussion emphasizes the low-Froude number flow. In addition, there are no investigations of the lee mesolow and the effect of rotation on the lee vortices in their study. They

find that no lee vortices form for a flow with Froude number larger than 0.5. This phenomenon is explained by the tilting of horizontal vorticity produced baroclinically in an inviscid fluid. However, Smith (1989b) comments that the lee vortices can be generated by either a density surface interaction or overturning and turbulence in an inviscid fluid. In the real atmosphere, once the stagnation point forms, the flow tends to be turbulent and the boundary layer along the lateral slope of the mountain may separate. In a recent study, the upwind flow reversal and effects of mountain shapes have been examined by Smolarkiewicz and Rotunno (1990).

Idealized numerical experiments of low-Froude number flow past a bell-shaped mountain have also been performed by Crook et al. (1991) recently. When the Froude number decreases, the flow aloft over the lee slope reverses. Wave breaking then follows and the region of flow reversal descends to the surface. In this way, the lee vortices are able to form near the surface. Thus, they suggested that the intense, concentrated vorticity that develops in the lee of obstacles at low-Froude numbers is due to the tilting of horizontal vorticity as gravity waves overturn and break. It appears that this argument is a merger of the theories proposed by Smith (1989b) and Smolarkiewicz and Rotunno (1989a). However, Rotunno and Smolarkiewicz (1991) indicated that the wave breaking aloft over the lee slope should be viewed as a separate phenomenon from the lee-vortex formation since the lee vortex forms before the lee wave breaks when the flow is accelerated gradually from rest. Therefore, Rotunno and Smolarkiewicz concluded that a theory for lee-vortex formation is not yet in hand. It will also be shown in this study that some inconsistencies still exist among the numerical results and existing theories.

For inviscid flow over Hawaii, Smolarkiewicz et al. (1988) found that a pair of lee vortices form on the lee side of the island, which then shed downstream at later times. They offer no explanation for his behavior in that study. The same phenomenon is not found in the study of Smolarkiewicz and Rotunno (1989a). However, Smolarkiewicz and Rotunno suggest that the shedding of lee vortices may be due to the asymmetry of the mountain shape. This problem needs to be clarified in order to understand the dynamics of orographically-induced mesovortices.

A careful inspection of the analysis of TAMEX data (e.g., Kuo and Chen, 1990, also see Figs. 1c and d) suggests that the southeast Taiwan mesolow is not necessarily coupled with a mesovortex. Thus, the formation mechanisms of the orographically-induced mesolow and mesovortex may be different and deserve a fundamental study. As mentioned earlier, the typical speed for a southwesterly flow is about 5 to 15 ms^{-1} and the CMR extends to a height of 4 km. Thus, the Froude number falls into the range of 0.125 to 0.375. Since the nonlinearity is proportional to the reciprocal of the Froude number (i.e., Nh/U, Smith, 1980), the flow is highly nonlinear. Therefore, we will use a nonlinear numerical model to investigate the formation and development of lee mesolows and mesovortices. The nonlinear effects will be investigated by comparing the strengths of the lee mesolows and vortices for flow over mountains with different heights but keeping the Froude number constant. Since the CMR has a width of about 120 km and a length of about 300 km, the effect of planetary rotation may modify the flow to a certain extent. Thus, rotational effects on the formation of lee mesolows and mesovortices need to be investigated.

Figures 1c and d also indicate that the mesolow located to the east of Taiwan is colocated with the cyclonic vortex. This combined mesolow and closed cyclonic circulation may be regarded as a mesocyclone. In fact, earlier observations do show some cases of lee cyclogenesis over the eastern side of the CMR of Taiwan (TAMEX, 1985). In a recent numerical study of an inviscid low-Froude number flow over eastern Colorado, it is found that a mesocyclone forms over the Denver region (Denver Cyclone) and moves downstream (Crook et al., 1990). A similar phenomenon may occur for flow over the CMR. However, Crook et al. found that the flow in the lee of the Palmer Divide is not significantly affected by the earth's rotation. Even though the formation mechanism of the lee vortex is reasonably explained in their study, the formation of the lee mesolow associated with the lee vortex (i.e., the mesocyclone) remains to be explained.

Possible mechanisms for producing lee mesolows and mesovortices will be reviewed briefly in section 2. In section 3, we will present numerical results for flow past an idealized topography with a Froude number which varies from 0.125 to 1.5.

Attention will be drawn to the formation mechanisms of the lee mesolows and the development of lee mesovortices and mesocyclones. Both rotational and slope effects will be investigated. In section 4, we will present results of flow over the real topography of Taiwan. The Taiwan mesolow problem will be discussed within the context of the plausible mechanisms discussed in section 2. Finally, conclusions and suggestions for further studies of the mesolow problem are made.

2. Brief Review of Formation Mechanisms of Lee Mesolows and Mesovortices

The following mechanisms which will be reviewed and discussed are suggested as plausible formation mechanisms of lee mesolows and mesovortices: (a) boundary layer separation, (b) baroclinic vorticity tilting/potential vorticity generation, (c) mountain waves, and (d) planetary vorticity stretching.

2.1 Boundary Layer Separation

The most appealing mechanism for explaining the lee vortices and mesolows is the boundary layer separation which is a well-known phenomenon in experimental fluid dynamics. For a steady, homogeneous flow past a circular cylinder at high Reynolds number, the streamlines passing the upstream side of the cylinder break away at both lateral sides of the cylinder and enclose fluid in a slow and unsteady motion (Batchelor, 1967). A stagnation point and a pair of cyclonic and anticyclonic vortices form on the upstream and lee sides of the cylinder, respectively. The right (left) vortex, if one faces downstream, has a positive (negative) vorticity. In the mean time, low pressure centers on the lateral sides of the cylinder are carried downstream with the vortices. Thus, the lee vortices associated with the mechanism of boundary layer separation should have low pressure associated with them no matter whether the flow circulation is cyclonic or anticyclonic. At higher Reynolds numbers, the flow becomes transient and vortex shedding may occur.

For a three-dimensional flow past real topography, such as the CMR, one should consider the additional effects of stratification, wave breaking, turbulence, and vertical wind shear (for a review, see Smith, 1989a). In addition, the results of tank experiments may not be directly applicable to the real atmosphere because the laboratory investigations in water tanks are still plagued by the need to use generally low Reynolds numbers and an exaggerated model height-to-width ratio (Smith, 1989a). For example, it has been documented that the atmospheric boundary layer developing over most natural surfaces is characterized by very large (10^6–10^9) Reynolds numbers (Arya, 1988). Nonetheless, one should be able to obtain a qualitative picture from the above results. For a southwesterly flow past the CMR, the theory of boundary layer separation predicts that a pair of lee vortices forms to the northwest and southeast of Taiwan. These vortices may shed downstream if the Reynolds number is large enough. The location of this southeast vortex and the associated cyclonic circulation seem to be consistent with observations (Fig. 1).

For flow past the CMR of Taiwan, one may anticipate that the boundary layer separation will occur on both lateral slopes as well as on the vertical plane. Using a horizontal resolution of 10 km, Huang and Raman (1990) have shown that the results obtained from the addition of the planetary boundary layer does not differ significantly from the inviscid flow results. Similar results have been found in the numerical simulation of the Denver Cyclone (Crook et al., 1990). However, the most challenging problem in testing this mechanism in a mesoscale numerical model is that the grid resolution should be fine enough to resolve the turbulent eddies which often have a scale on the order of one hundred meters.

2.2 Baroclinic Vorticity Tilting/Potential Vorticity Generation

In a numerical modeling study, Smolarkiewicz and Rotunno (1989a, b) show that a pair of lee vortices may form in an inviscid, stratified flow past a three-dimensional bell-shaped mountain when the Froude number ($Fr = U/Nh$) is smaller than 0.5. These vortices tend to remain stationary on the lee slope after a nondimensional time $Ut/a = 3$. They explain that the vertical vorticity in the vortex couplet derives from the tilting of horizontal vorticity produced baroclinically as the isentropes deform in response to the flow over the obstacle. Their argument is based on the second-order steady state equation of the vertical vorticity (ζ_2)

$$u_0 \frac{\partial \zeta_2}{\partial x} = \xi_1 \frac{\partial w_1}{\partial x} + \eta_1 \frac{\partial w_1}{\partial y}, \quad (1)$$

$$\xi_1 = \frac{1}{u_0} \int_{-\infty}^{x} \frac{\partial b_1}{\partial y} dx, \quad (2)$$

where u_0 is the basic wind velocity, w_1 the first-order vertical velocity, b_1 the first-order buoyancy, ξ_1 and η_1 the first-order x and y vorticities, respectively. On the right side of the upstream slope, if one faces downstream, a negative x-vorticity (ξ_1) is generated due to relatively colder air from adiabatic upslope ascent at the center line ($\partial b_1/\partial y > 0$) according to Eq. (2). This negative x-vorticity is then carried over to the downstream slope by advection of the basic current and tilted in the vertical direction according to Eq. (1). For $Fr < 0.5$, flow stagnation occurs on the upstream slope and a pair of vortices form on the lee side of the mountain. For a typical flow past the CMR with $5\,\mathrm{ms}^{-1} < U < 15\,\mathrm{ms}^{-1}$, $N = 0.01\,\mathrm{s}^{-1}$, and $h = 4\,\mathrm{km}$, the Froude number is in the range 0.125–0.375. Thus, a stagnation point may form when a typical flow impinges the CMR. This theoretical analysis is also consistent with observations (Fig. 1).

Smith (1989b) comments that the generation of lee vortices, such as those found by Smolarkiewicz and Rotunno, requires a violation of Ertel's theorem or the corresponding circulation theorem and is not just nonlinear behavior of the mountain wave field. Instead, the lee vortices can be generated by either (i) a density surface interaction or (ii) overturning and turbulence in an inviscid stratified flow, instead of through the vorticity tilting. The first mechanism suggests that when an inviscid stagnation point forms and density surfaces intersect the mountain, a no-slip condition at the boundary forces the generation of potential vorticity. The second mechanism suggests that once fluid overturning and turbulence occur, a recirculation region near the lower boundary forms on the upstream slope. The potential vorticity created in this region is then carried into the wake near the lower boundary. The overturning and turbulence can also occur in the wave-breaking region aloft. Notice that these two mechanisms may not be distinguishable and may not be independent of the boundary layer separation (Smith, 1989a, b). Based on this theory of lee eddies, Smith makes three predictions: (i) lee eddies are possible only after a surface stagnation point forms upslope, (ii) every closed contour (C) lying in a density surface (S) with nonzero isosteric circulation ($\Gamma \neq 0$) must have either a region of nonzero potential vorticity (PV) inside (on S) or be irreducible (a collapsed region inside), (iii) the condition for the formation of lee eddies begins suddenly, with the onset of the upslope stagnation point, rather than progressively as the mountain waves become more and more nonlinear. Smolarkiewicz and Rotunno's simulations confirm the first point, but find that it is difficult to compute PV near the lower boundary. However, an investigation of the third point may serve as a test of the theory.

In applying the above mechanism to the flow past the CMR during the Mei-Yu season, one may expect a pair of vortices to form to the southeast and northeast of Taiwan in a prevailing southwesterly flow before the passage of the Mei-Yu front and a pair of northwest and southwest vortices in a prevailing northeasterly flow behind the Mei-Yu front. However, due to the disagreement between Smolarkiewicz and Rotunno (1989a) and Smith (1989b), the interpretation of the generation mechanism of the lee vortices as simulated by Smolarkiewicz and Rotunno still needs to be resolved by further work. Again, one should keep in mind that the lee vortex does not necessarily produce mesolows with it.

2.3 *Linear Mountain Waves*

For a nonrotating buoyancy-dominated hydrostatic flow over an isolated two-dimensional ridge, upward propagating gravity waves are generated (Queney, 1947). Associated with these hydrostatic mountain waves are high and low pressure regions located upstream and downstream of the mountain, respectively. Smith (1980) has extended the linear theory of Queney to three-dimensional flow over an isolated mountain. The streamline pattern associated with this high-Froude number flow exhibits no closed anticyclonic and cyclonic circulations around the high and the low, respectively. However, the high-low pressure pattern has also been observed over mesoscale mountains such as the New Zealand Alps, Iceland, the Front Range of the Rockies, and Taiwan's CMR (Smith, 1982).

For flow past a mesoscale mountain with Rossby number of $O(1)$ or smaller, the rotational effect becomes more important and cannot be ignored. As an air parcel approaches a mesoscale mountain, it is decelerated by the mountain-induced high pressure and the flow becomes subgeostrophic. The slower moving parcel feels a decreased Coriolis force and it thus begins to curve to the left (in the Northern Hemisphere) under the influence of the background pressure gradient (Smith, 1982). Numerical simulations of a three-dimensional inviscid flow past an isolated mountain with $Ro = 1$ also indicate a left-turning of air parcels upstream of the mountain (Thornsteinsson, 1988). The low pressure on the lee side is produced by the downslope wind associated with the upward propagating inertia-gravity waves through adiabatic warming. For a typical southwesterly flow, the linear theory of Smith (1982) predicts the formation of a low to the northeast of Taiwan. However, the low may be shifted to the southeast of Taiwan through the nonlinear and rotational effects in a low-Froude number flow. It is important to mention that the Taiwan mesolow is not necessarily associated with closed circulations (vortices), such as the southeast low shown in Fig. 1c.

2.4 Planetary Vorticity Stretching

In a homogeneous incompressible fluid, the conservation of potential vorticity ($(\zeta + f)/\delta z = \text{constant}$) implies that cyclonic vorticity can be generated if a cylindrical air column stretches as it passes over the mountain top and descends to the lee side.

As mentioned above, most of the low-level flow is blocked by the CMR because of the low Froude number (0.125–0.375). The air parcels located on top of the mountain tend to descend on the lee side. Based on this, Kuo and Chen (1990) proposed that a cyclonic vorticity center may form on the lee side through the air column stretching.

With upstream blocking and wave breaking in stratified flow, Ertel's (1942) theorem, which expresses the conservation of potential vorticity for adiabatic flow is violated (Smith, 1989a). In addition, the rotational effect may not be significant enough to produce a lee vortex for a flow over a mesoscale mountain compared with that over a large scale mountain (e.g., see Thornsteinsson, 1988). The effects of planetary rotation on the formation and development of lee vortices deserves investigation. Notice that the Rossby number for a typical southwesterly flow past Taiwan is on the order of 1. Air parcels which pass around the mountain and inertia-gravity waves generated above the mountain may also modify the formation and development of the vorticity generated by the air column stretching. In addition, it is important to note that the vorticity stretching can only contribute to the later development of the lee vortices, but cannot contribute to their initial formation, according to the vorticity equation.

The objectives of this study are to investigate the formation and development of lee mesolows, mesovortices, and mesocyclones. Then the proposed mechanisms as outlined above will be applied to the problem of the Taiwan mesolow. The nonlinear and rotational effects on the mesolow and mesovortex will also be discussed.

3. Flow over Idealized Topographies

The Colorado State University RAMS cloud/mesoscale model is used to perform the numerical experiments (Tripoli and Cotton, 1982). For this study, we have assumed a hydrostatic atmosphere on a terrain-following sigma-z vertical grid. The vertical model domain is 10 km and the vertical grid interval is 500 m. The horizontal domain is 400 km by 400 km . The grid interval is 10 km in both x and y directions. The time step used in all simulations is 15 s. The moisture variables, such as water vapor, cloud, rain, ice crystal, and graupel remain zero throughout the simulations. At the lateral boundaries, we have used the Orlanski radiation boundary condition (Orlanski, 1976). A mesoscale compensation region (MCR, for details see Tripoli and Cotton, 1982) of width equal to the domain width is used. The MCR is a large grid box placed outside the simulation domain, which will keep track of mass leaving and entering the domain at each vertical level. Compensating lateral and vertical motion will occur in the MCR which will, in turn, feed back on the simulation domain. On the upper boundary, we have used the Klemp-Durran radiation boundary condition (Klemp and Durran, 1983). For all simulations, the exchange coefficients of momentum and heat are set equal to zero. However, a fourth-order numerical smoother is applied, which may include viscous effects impli-

Table 1. *Summary of Numerical Experiments with Idealized Topographies*

Case	I1	I2	I3	I4	I5	I6	I7
Fr	0.125	0.125	0.125	0.25	0.5	1.0	1.5
h (km)	4	4	2	2	2	2	2
U (ms^{-1})	5	5	2.5	5	10	15	20
f (s^{-1})	0	5.8×10^{-5}	0	0	0	0	0
a (km)	50	50	50	50	50	50	50

citly. In this study, we have used the Exner function (i.e., $\pi = c_p(p/p_{00})^{R/c_p}$) for the pressure disturbance, where c_p is the specific heat capacity of air at constant pressure, p the pressure, p_{00} is 1000 mb, and R the universal gas constant for dry air. The perturbation Exner function is approximately related to the perturbation pressure by $\pi' = (R_d/p_{00})p'$. Thus, a perturbation of 1 mb is approximately equal to $0.287\,J\,kg^{-1}\,K^{-1}$. The detailed description of numerical techniques incorporated into the model can be found in Tripoli and Cotton (1982). Several numerical experiments are performed in this study, which may help to understand the formation of lee mesolows, transient features of lee vortices, effects of planetary rotation and mountain slope on flows with different Froude numbers past idealized topography. Table 1 summarizes the following experiments on the basis of Froude number, mountain height, basic flow speed, and Coriolis parameter.

In the following numerical experiments, we will consider an inviscid, continuously stratified flow past a circular bell-shaped mountain, i.e.

$$h(x, y) = \frac{h}{(x^2/a_x^2 + y^2/a_y^2 + 1)^{3/2}} \tag{3}$$

where a and h are the mountain's horizontal scale and maximum height, respectively. In all simulations, the constant lapse rate is assumed to be $6.5\,°C\,km^{-1}$. The initial pressure field is diagnosed from the geostrophic wind relation at each level. The bell-shaped mountain, which cuts through the atmosphere without modifying the initial fields, is then introduced. The Brunt-Vaisala frequency is $0.01\,s^{-1}$ in all cases.

3.1 *Control Case (Case I1)*

In the beginning, we consider a nonrotating flow with a very low Froude number of 0.125. The basic wind speed is $5\,ms^{-1}$. The mountain height (h) and horizontal scale (a) are 4 km and 50 km, respectively. A mountain height of 4 km is used since we are interested in the flow over the CMR of Taiwan whose highest peak is about 4 km. The Coriolis parameter is set equal to zero. Figure 2 shows the streamlines, perturbation pressure, and vertical velocity on the 250 m surface, and vector wind on the vertical plane at $y = -5$ km after a nondimensional time $Ut/a = 3.6$. The corresponding dimensional time is 10 h. On the upstream side of the mountain, a nodal (attachment) point forms near the surface at about $x = -30$ km (Fig. 2a). It can be seen from the vector wind field on the vertical plane at $y = -5$ km that some air parcels tend to go over the mountain, while others recirculate from the attachment point back upstream near the surface. The recirculated air parcels meet the incoming air parcels at the saddle (stagnation) point which is located upstream of the left boundary. A significant portion of the air parcels are forced to go around the mountain (Fig. 2a). A region of upward motion forms above the mountain peak near $(x, y) = (25\,km, 4\,km)$, which is associated with the mountain waves over the lee slope. Two vortices form on the lee side of the mountain at about $x = 120$ km (Fig. 2a). The horizontal scale of the vortices is about 50 km which falls into the mesoscale. The circulations associated with these two mesovortices are opposite. The right vortex (facing downstream) has a cyclonic circulation, while the left vortex has an anticyclonic circulation. The formation mechanism of the lee mesovortices will be explained later. The flow structure associated with the lee vortices is consistent with that of Smolarkiewicz and Rotunno (1989a) and resembles the sketch of Smith (1989a). However, unlike the finding of Smolarkiewicz and Rotunno (1989a), this pair of lee vortices is transient as will be shown later.

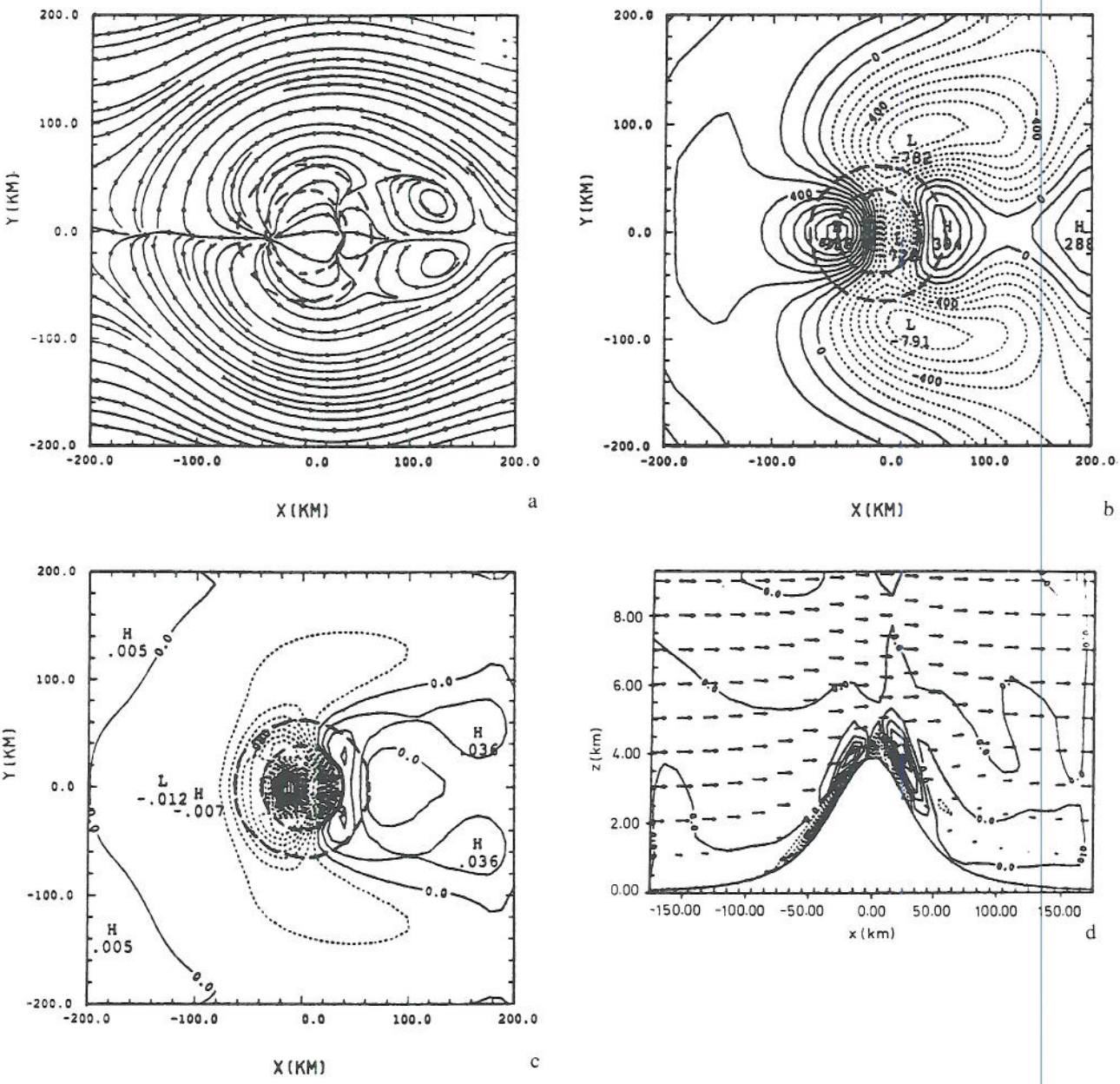

Fig. 2. (case I1) An inviscid stratified nonrotating flow over a circular bell-shaped mountain after $Ut/a = 3.6$ (10 h). The Froude number is 0.125. The basic wind speed and Brunt-Vaisala frequency are $U = 5\,\mathrm{ms}^{-1}$ and $N = 0.01\,\mathrm{s}^{-1}$. The mountain height and half-width are 4 km and 50 km, respectively. Contours of 1000 and 2000 m of the mountain are depicted by heavy dashed curves. Four fields are shown: (a) streamlines on 250 m surface, (b) perturbation pressure (Exner function, contours from -0.23 to $0.05\,\mathrm{J\,kg}^{-1}\,\mathrm{K}^{-1}$), (c) vertical velocity on 250 m surface (contours from -0.28 to $0.06\,\mathrm{ms}^{-1}$), (d) vector wind and vertical velocity on the vertical plane at $y = -5$ km. A stagnation point forms upstream and two vortices form on the lee side of the mountain

On the lee side, one convergence point forms at about $x = 30$ km and one stagnation point forms at $x = 160$ km. Near $x = 40$ km, there exists a region of wave steepening as depicted in Fig. 2c. This region of upward motion is associated with convergence formed by the downslope wind and the return flow. A mesohigh pressure forms upstream with the maximum located at $x = -40$ km and a mesohigh also forms on the lee side of the mountain. Three local low pressure maxima also form to the north, south and upstream of the lee mesohigh. With the Scorer parameter (N/U) of $2 \times 10^{-3}\,\mathrm{m}^{-1}$ and the horizontal wave number ($2\pi/50$ km) of $1.2 \times 10^{-4}\,\mathrm{m}^{-1}$, the flow falls into

the regime of upward propagating gravity waves. However, the gravity waves above 5 km are very weak since most of the fluid particles split upstream and pass around the mountain. The upstream high and the lee slope low can be explained by the hydrostatic mountain wave theory since the model assumes a hydrostatic atmosphere. The upstream high pressure is located near the upstream stagnation point and the major lows are located at $x = 20$ km. It can be shown that the pressure perturbations in a hydrostatic atmosphere can be formed either (a) by the vertical motion through thermodynamic energy conservation, or (b) by the convergence/divergence associated with momentum conservation. In the present case, the low on the lee slope is mainly produced by the downslope wind associated with upward propagating gravity waves through adia-

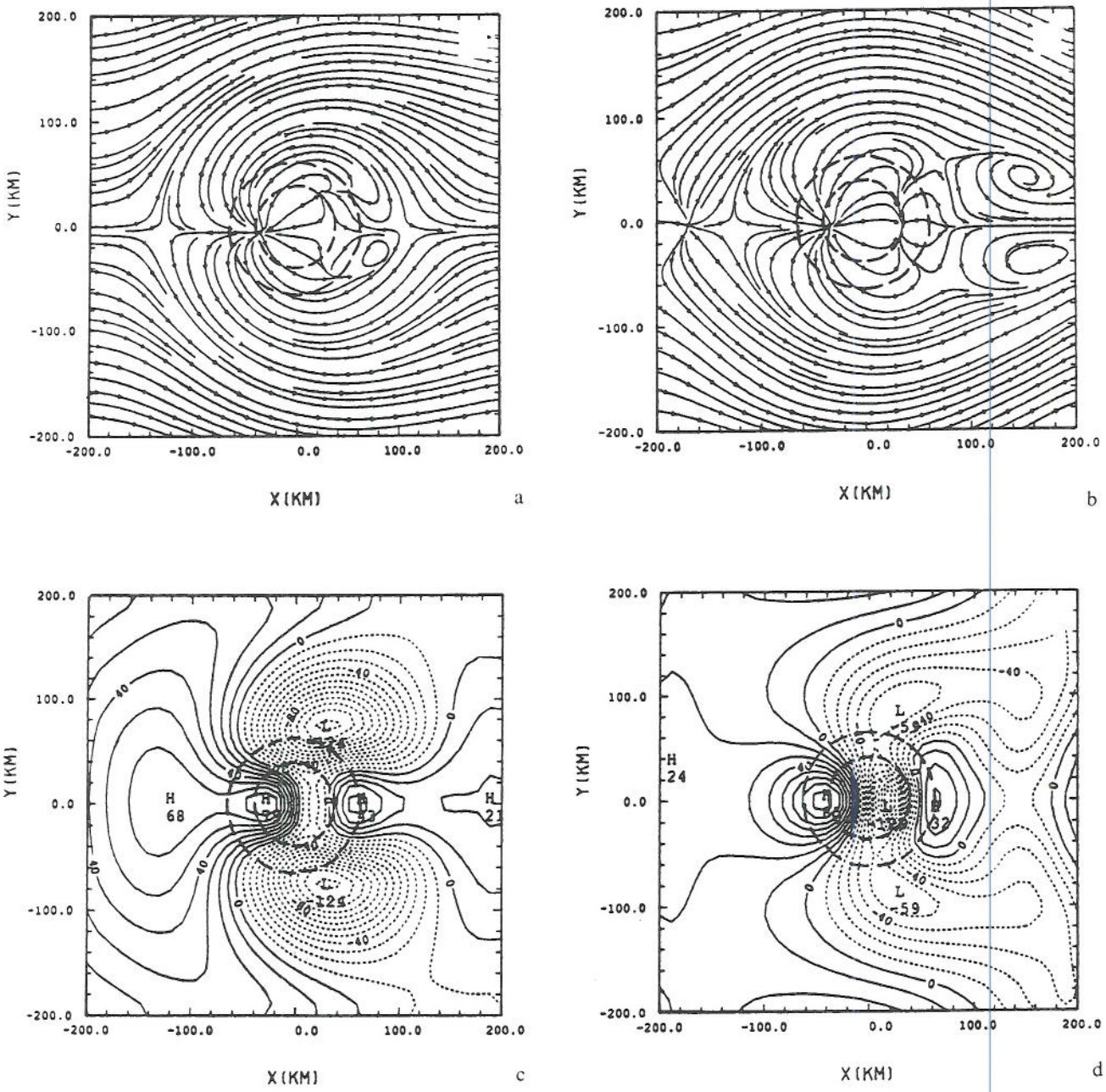

Fig. 3. Streamlines for the flow of Fig. 2 after (a) $Ut/a = 1.8$ (5 h) and (b) $Ut/a = 5.4$ (15 h). The corresponding pressure perturbations are shown in (c) and (d)

batic warming. However, the high pressure and two other weak local low pressure centers on the lee side of the mountain are formed mechanically by convergence/divergence through the momentum equation since the vertical motion is very weak there. This is because the vertical motions there are too weak to produce enough density perturbation through the thermodynamic energy equation (Fig. 2c). The results also indicate that the mesolow does not necessarily collocate with the lee mesovortices. The anticyclonic circulation of the left vortex, if one faces downstream, also indicates that the vortex formation is not due to the vorticity stretching mechanism as proposed by Kuo and Chen (1990).

To investigate the transient features of the flow, we display the streamline patterns and pressure perturbations at $Ut/a = 1.8$ and 5.4 ($t = 5$ and 15 h) in Fig. 3. One interesting and important finding is that the lee vortices in this case are not

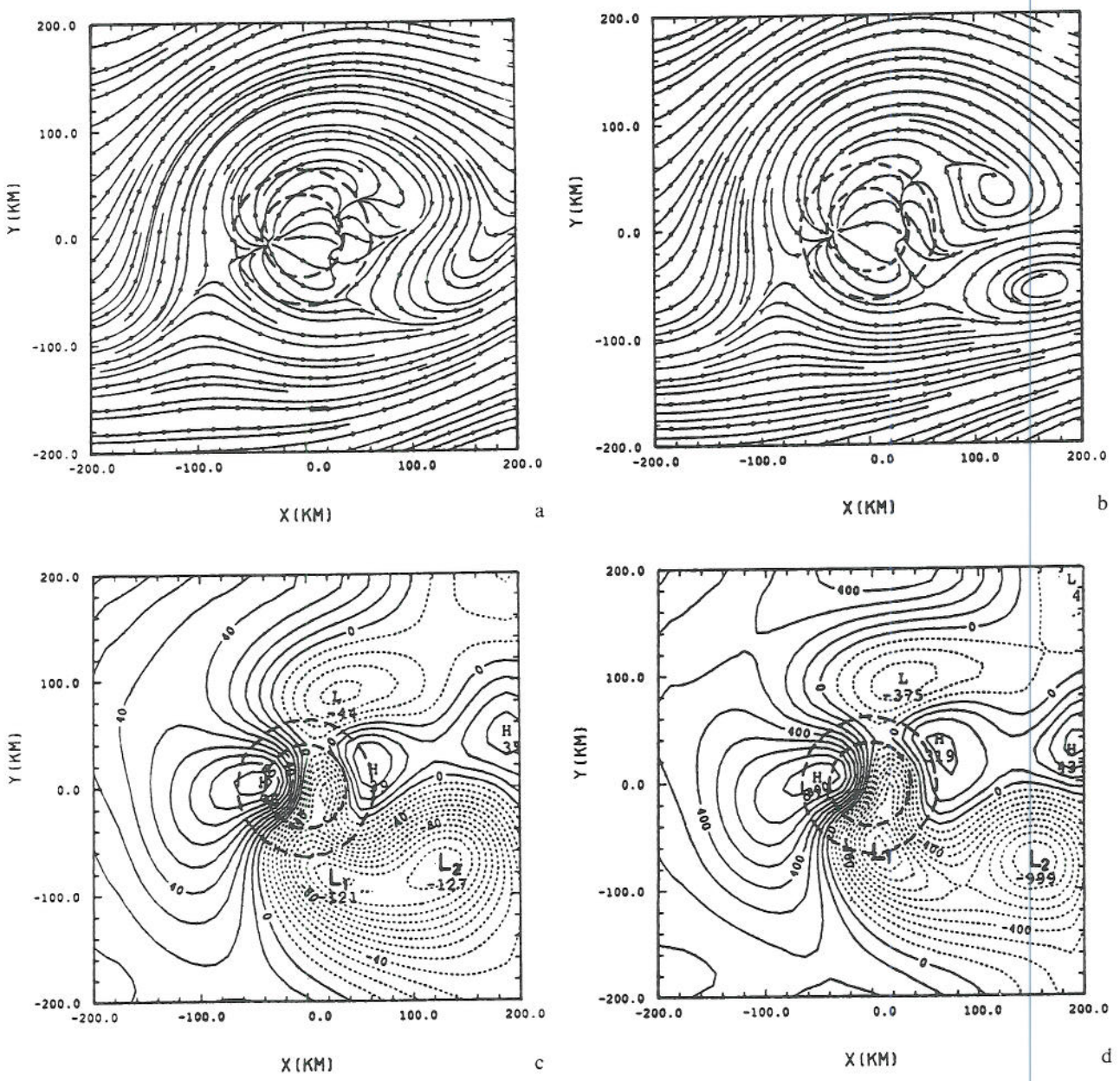

Fig. 4. (case I2) Streamlines for the same flow of Fig. 2 except with the addition of planetary rotation: (a) $Ut/a = 3.6$ and (b) $Ut/a = 5.4$. The Coriolis parameter and Rossby number are $5.8 \times 10^{-5}\,s^{-1}$ and 1.72, respectively. The symbols L_1 and L_2 denote the lee mesolow and lee mesocyclone, respectively. The corresponding pressure perturbations are shown in (c) and (d)

steady as those found in Smolarkiewicz and Rotunno (1989a), but rather transient. At $Ut/a = 1.8$, two stagnation points form on the downstream slope (Fig. 3a). A pair of weak lee mesovortices forms at $x = 80$ km, although the northern vortex is not as pronounced as the southern one. At $Ut/a = 3.6$, a pair of cyclonic and anticyclonic vortices form on the lee side at about $x = 120$ km (Fig. 2a). This pair of lee vortices moves downstream, strengthens, and then weakens at later times (Fig. 3). The downstream shedding of the lee vortices is similar to the results of Smolarkiewicz et al. (1988) for an inviscid flow past Hawaii. Smolarkiewicz and Rotunno (1989a) claim that the vortex shedding in that paper is due to the asymmetry of the mountain shape. However, the mountain shape in this experiment is symmetric, but the lee vortices still shed downstream. There exists a reversed pressure gradient just upstream of the vortices, which reduces the advection speed of the lee vortices to 3.3 ms^{-1}, i.e. about 2/3 of the basic wind speed of 5 ms^{-1} (Fig. 3b). This result is similar to that found in the numerical simulations of the Denver Cyclone (Crook et al., 1990). At $Ut/a = 1.8$, two mesolows form on the lee slope but are located to the north and south of the center line ($y = 0$). At $Ut/a = 3.6$, a third mesolow forms on the lee slope at $(x, y) = (20, 0$ km), which then develops to be the major mesolow at later times such as $Ut/a = 5.4$ (Fig. 3). Thus, the mesolow persists and remains on the lee slope at the same location, while the mesoscale vortices tend to shed downstream.

3.2 *Rotational Effects (Case I2)*

Figure 4 shows the streamlines and pressure perturbations at $Ut/a = 3.6$ and 5.4 for the same flow of case I1 (Fig. 2) except with the planetary rotation (Coriolis force) included. A Coriolis parameter of $5.8 \times 10^{-5}\ s^{-1}$ is used since we are interested in the Taiwan mesolow problem and because the island is centered at roughly 23.5° N. The flow becomes asymmetric compared with the nonrotational case (Case I1, Fig. 4). A significant portion of the fluid particles turn to the left on the upstream side of the mountain. This can be explained by the reversed pressure gradient on the upslope, which then requires a left turning (facing downstream) by the imbalance of the incoming geostrophic wind (Smith, 1982). The attachment point and stagnation point on the upstream slope are still evident at both $Ut/a = 3.6$ and 5.4, although the latter is formed to the south of the center line.

Unlike the nonrotating case (Fig. 2), the lee vortices do not form until $Ut/a = 3.6$ (Fig. 4a). This is caused by the left turning of the incoming flow. However, a pair of lee vortices do form and move downstream at later times (Fig. 4b). At $Ut/a = 5.4$, the circulation associated with lee vortices becomes asymmetric. It appears that the cyclonic vortex forms earlier and then moves farther downstream compared with the anticyclonic vortex. There exist two low pressure centers (L_1 and L_2) embedded in the low pressure region to the southeast of the mountain. The low pressure center located on the lee slope (L_1) appears to be associated with the lee mesolow as found in the nonrotating case (Fig. 2), which is formed by the downslope wind through adiabatic warming. However, another low pressure center located farther downstream (*L2*) is colocated with the cyclonic flow at $Ut/a = 3.6$ and with the mesovortex center at $Ut/a = 5.4$. Therefore, this advecting mesovortex may be regarded as a lee mesocyclone since it is characterized by cyclonic circulation with a low pressure region in a continuously stratified rotating fluid. The formation of the low pressure associated with the mesocyclone (*L2*) may be explained by combining the horizontal momentum equations to yield the divergence equation

$$\frac{D}{Dt}(u_x + v_y) - f(v_x - u_y) = -\frac{1}{\rho_0}\nabla_H^2 p \tag{4}$$

Near the vortex center, the second term on the left hand side dominates because the divergence term is very small. Thus, the above equation reduces to

$$\nabla_H^2 p = \rho_0 f(v_x - u_y) \tag{5}$$

Therefore, the cyclonic circulation tends to produce a low pressure. This type of lee mesocyclone may be related to the lee cyclogenesis in Taiwan (TAMEX, 1985) and other major mesoscale mountain ranges such as the Alps.

3.3 *Slope Effects (Case I3)*

To investigate the slope effect, we make a simulation identical to case I1 (Fig. 2) except with a lower mountain ($h = 2$ km) and a slower basic wind speed ($U = 2.5\ ms^{-1}$). Thus, the Froude number is kept the same (0.125). Since the strength of the non-

linearity is proportional to the reciprocal of the Froude number Nh/U (Smith, 1980), the present flow should have the same strength of nonlinearity as case I1.

Figure 5 shows the streamlines, perturbation pressure, and vertical velocity on the 250 m surface, and the vector wind and vertical velocity on the vertical plane at $y = -5$ km after $Ut/a = 3.6$. Although there exist attachment and stagnation points on the upstream slope near the surface (Fig. 5d), the disturbance appears to be shallower than the higher-mountain case (case I1) since these attachment and stagnation points do not appear on the 250 m surface (Fig. 5a). The recirculated flow on the upstream slope is much weaker than the higher-mountain case (Fig. 2). The lee vortices are located at the same place as in case I1, but with a weaker circulation and smaller overall horizontal extent. Even though the general features of the mesolows and vertical velocity are similar to the higher-mountain case (case I1), the lee mesolow is about 4 times and the vertical velocity is about 10

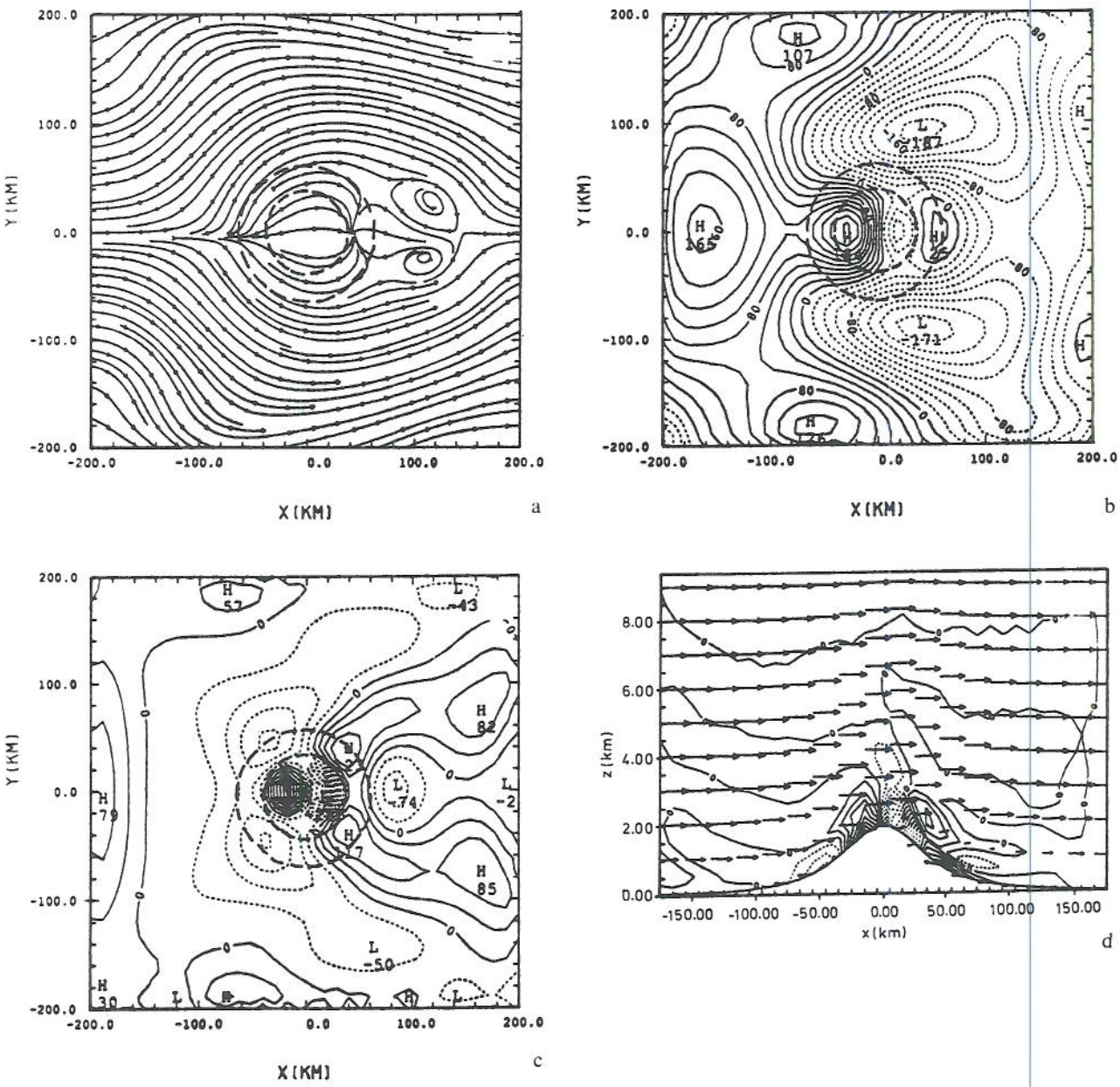

Fig. 5. (case I3) Same as Fig. 2 except with a mountain height of 2 km and a basic wind speed of 2.5 ms^{-1}. The contours of the mountain are depicted for 500 and 1000 m. The Froude number is 0.125

times weaker. In fact, the lee vortices in the present case (not shown) tend to weaken when they move farther downstream at later times. Therefore, we may conclude that a steeper mountain tends to produce a stronger disturbance if the Froude number and strength of nonlinearity are kept the same.

3.4 *Flows with Larger Froude Numbers (Cases I4, I5, I6, I7)*

Figure 6 shows the streamlines after $Ut/a = 3.6$ for flows with $Fr = 0.25$ (I4), 0.5 (I5), 1.0 (I6), and 1.5 (I7). For these flows, we keep the same mountain height (2 km) and vary the basic wind speed. Therefore, the results can be compared with case I3 and also with each other. For $Fr = 0.25$, a pair of lee vortices is formed on the lee side at about $x = 120$ km. This result is similar to the lower-Froude number flows (Figs. 2a and 5a). Unlike those cases, there is a saddle point, instead of a convergence point, formed just upstream of the lee vortices. There exists an attachment point and a saddle point on the upstream slope. For higher-Froude number flows (Figs. 6b, c, and d), the streamline patterns are similar to that predicted by linear

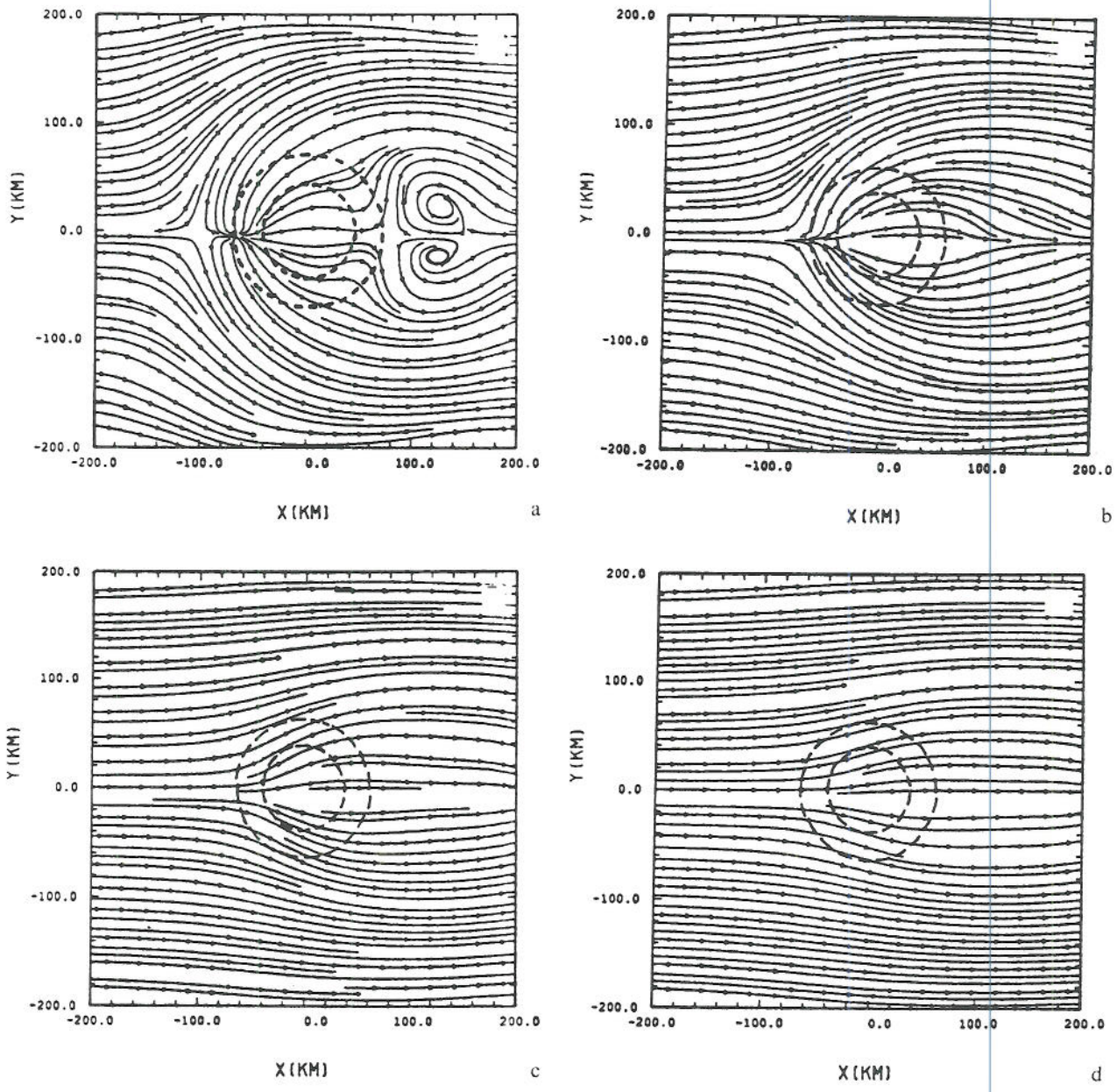

Fig. 6. Streamlines after $Ut/a = 3.6$ for flows with (a) $Fr = 0.25$ (case I4), (b) $Fr = 0.5$ (I5), (c) $Fr = 1.0$ (I6), and (d) $Fr = 1.5$ (I7)

theory (e.g., Smith, 1980) and those simulated by nonlinear models (Smolarkiewicz and Rotunno, 1989a). There is more flow splitting for a flow with $Fr = 0.5$ than those with $Fr = 1.0$ and 1.5.

Figure 7 shows the corresponding perturbation pressure on the 250 m surface for the flows of Fig. 6. For $Fr = 0.25$, a major mesohigh and a major mesolow form on the upstream slope and downstream slope, respectively. In addition, there is a mesohigh formed just downstream of the lee mesolow. This result is similar to the flow with $Fr = 0.125$ (Fig. 5b) except that the mesolow near the mountain peak is much stronger in the present case. For higher Froude number flows, a high pressure forms on the upstream slope and a low pressure on the downstream slope. Thus, there exists a pressure drag across the mountain. The pressure drag is higher for a higher-Froude number flow. This is consistent with the hydrostatic mountain wave theory. In all cases, there is always a mesolow formed on the downstream slope.

Figure 8 shows the corresponding wind vector and vertical velocity after $Ut/a = 3.6$ on the vertical plane of $y = -5$ km. There exists recirculated flow

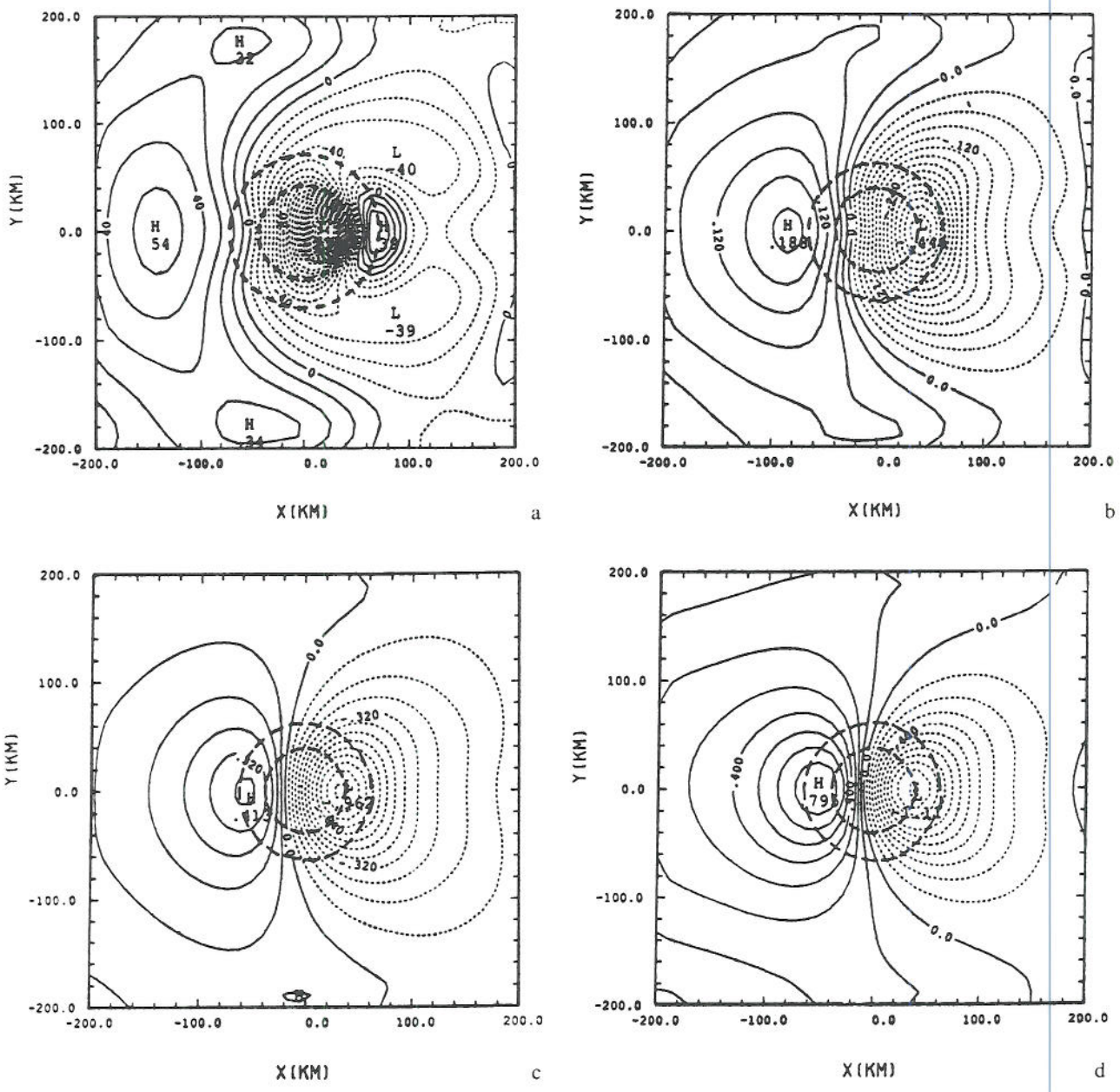

Fig. 7. Same as Fig. 6 except for perturbation pressure fields on 250 m surface

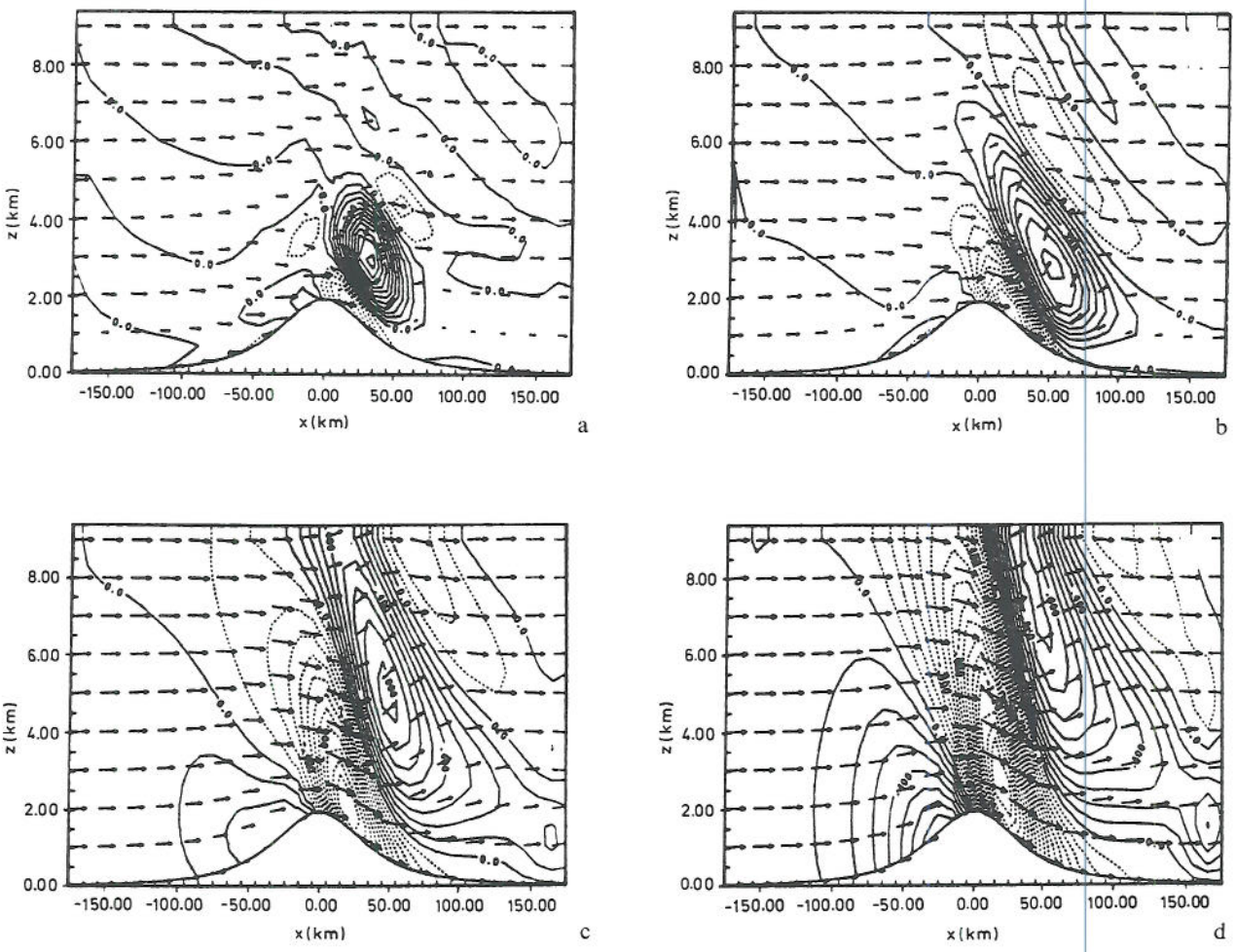

Fig. 8. Same as Fig. 6 except for wind vector and vertical velocity fields on the vertical plane at $y = -5$ km

near the upstream slope for flows with $Fr = 0.25$ and 0.5, while no such recirculated flow exists on the upstream slope for flows with $Fr = 1.0$ and 1.5. In all cases, the upward propagating gravity waves are evident in the vertical velocity fields. According to linear theory, the upward propagating hydrostatic mountain wave repeats itself in the vertical with a wavelength of $2\pi U/N$. Thus, a higher Froude number flow has a larger vertical wavelength if the mountain height is kept constant. Notice that there is no obvious evidence of air column stretching over the lee mesolow as proposed by Kuo Chen (1990). As discussed earlier, this lee mesolow is formed by the downslope wind through adiabatic warming, instead of through air column stretching.

From the wind vector fields at $Ut/a = 3.6$ on the vertical plane of $y = -5$ km, there exists a stagnation point on the upstream slope for flows with $Fr = 0.5$ (Fig. 8b). However, there are no lee vortices formed at this time (Fig. 6). To explore the possibility of the existence of lee vortices for a flow with $Fr = 0.5$, we make a longer simulation for case 15. Figures 9a and b show the streamlines and perturbation pressure on the 250 m surface after $Ut/a = 7.2$. A pair of lee vortices do form between $Ut/a = 5.4$ and 7.2. In other words, the lee vortices do not concur with the stagnation point on the upstream slope in time, but rather form at a later time. The formation of the lee vortices may be explained by the baroclinically-induced vorticity tilting as the mountain waves become more and more nonlinear. It appears that this formation mechanism is a merger of the theories proposed by Smith (1989b) and Smolarkiewicz and Rotunno (1989a). However, some inconsistencies still exist among the present numerical results and their theories. For example, the lee vortices do not concur with the upslope stagnation point in time as suggested by Smolarkiewicz and Rotunno

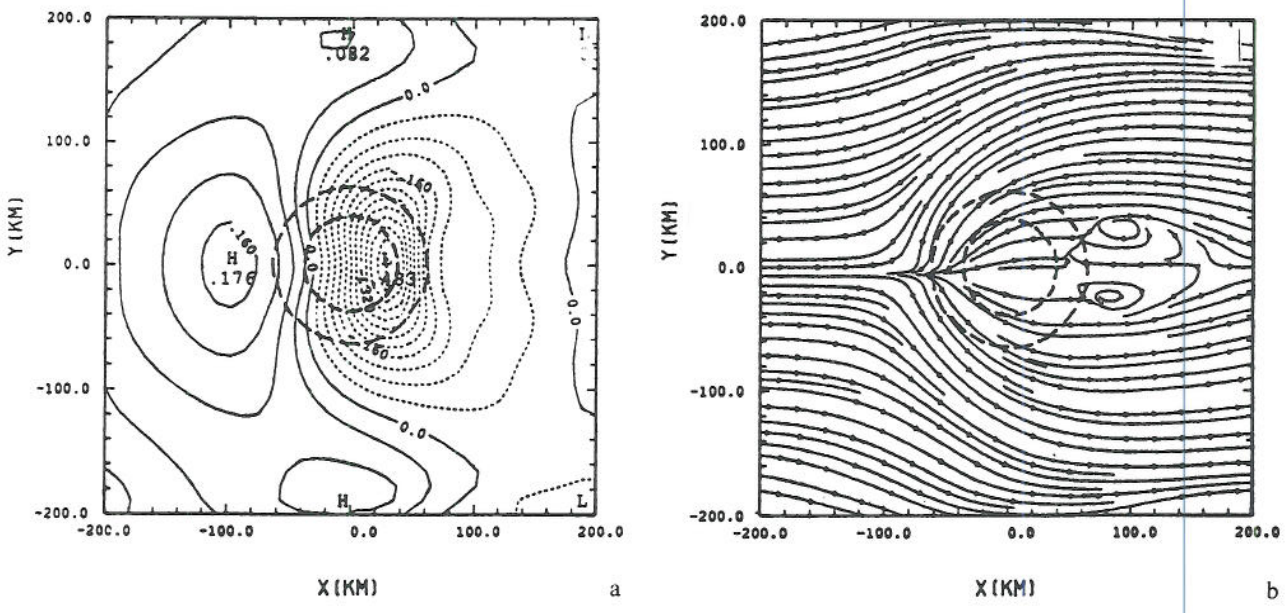

Fig. 9. (case I5) Streamlines and perturbation pressure on 250 m surface for a flow with $Fr = 0.5$ over a bell-shaped mountain after $Ut/a = 7.2$

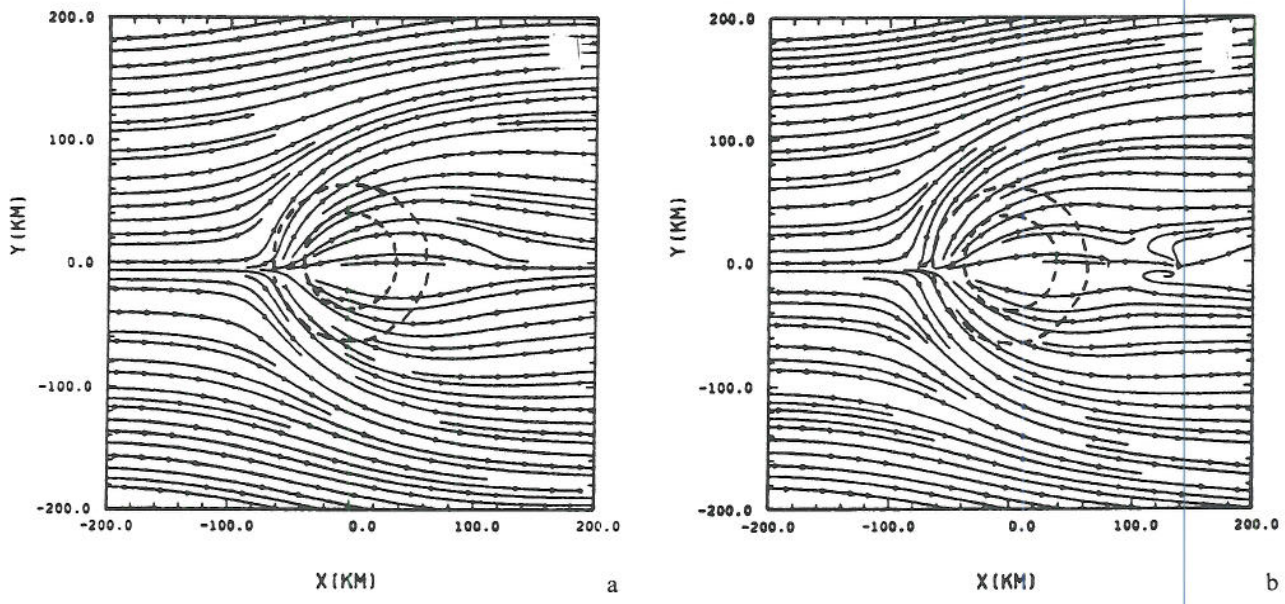

Fig. 10. Streamlines for a flow with $Fr = 0.66$ after $Ut/a = 7.2$ (a) and 10.8 (b). Notice that a pair of small-scale lee vortices is present downstream at $Ut/a = 10.8$, but not at 7.2

(1989a) and predicted by the lee eddy theory of Smith (1989b), but rather form at a later time. Our results also indicate that there exists no wave overturning and breaking over the lee slope (Figs. 2, 5, and 8). This result is different from that found in Crook et al. (1990). The lack of wave overturning and breaking may be viewed by a separate phenomenon from the lee-vortex formation (Rotunno and Smolarkiewicz, 1991). Further investigations are needed to resolve this problem.

To explore the possibility of the existence of lee vortices for flow with Froude number greater than 0.5, we make a simulation for a flow with $Fr = 0.66$ (Fig. 10). After $Ut/a = 7.2$, the streamlines are very similar to the flow with $Fr = 0.5$ (Fig. 6). However, a pair of relatively smaller scale lee vortices does

form at $x = 120$ km after $Ut/a = 10.8$. Another simulation with $Fr = 0.75$ (not shown) indicates that there exists a stagnation point on the upstream slope, but not for flows with $Fr \geqslant 1$ (Fig. 8). This is consistent with the prediction of Smith (1989c) who suggested that the critical Froude number is approximately 0.75 for a bell-shaped mountain with an aspect ratio of 1. Due to the smaller scale of the lee vortices generated in a moderately low Froude number ($0.5 < Fr < 1$) flow, finer grid resolution is needed to resolve structural details.

4. Flow over the real Topography of Taiwan

For flow simulations past the real topography of Taiwan, we assume a 400 km by 800 km domain on a planetary f-plane since the CMR is elongated in the y-direction. The grid interval in the x- and y-directions is equal to 10 km by 20 km, respectively. Specific parameters for the numerical simulations are given in Table 2. These include the Froude number, basic wind speed, impinging angle of the flow, and the Coriolis parameter. Otherwise, the parameters for this series of numerical simulations are the same as for the idealized topography cases. The magnitude of the basic flow is $5\,\mathrm{ms}^{-1}$. Thus, the Froude number is about 0.125 since the height of the CMR is 4 km. The Coriolis parameter is set to $5.8 \times 10^{-5}\,\mathrm{s}^{-1}$ since the center of the island is located at roughly 23.5° N.

4.1 Southwesterly Flow Past CMR (Case T1)

Figure 11 shows the flow fields after 10 h for an inviscid, continuously stratified southwesterly flow past the real topography of Taiwan. Although the upstream flow splits around the island, there are no stagnation points formed upstream and no vortices formed on the lee side of the CMR. The downslope wind on the upstream slope is relatively weak. This is because the impinging angle of the basic flow on the CMR is small. The perturbation pressure field (Fig. 11b) shows a strong pressure gradient across the mountain range. A mesohigh forms to the west of the CMR, while a major mesolow forms to the southeast. The lee mesolow is shifted to the southeast by the earth's rotation, which is similar to case I2 (Fig. 4). As in the idealized simulations, the upstream high and the leeside mesolow can be explained by hydrostatic mountain wave theory. The low is formed mainly by the downslope wind associated with mountain waves through adiabatic warming. Since the flow is highly nonlinear, the downstream mesolow is strengthened by the stronger downslope wind, while the upstream mesohigh is weakened by the recirculated flow near the surface.

The upward motion is very sensitive to the local features of the real topography. There exist two regions of maximum upward motion formed upstream of the two peaks of the CMR. A region of weak upward motion forms to the east of the CMR (Fig. 11c), which is dictated by the flow convergence imposed by the momentum equation. Descending motions exist elsewhere on the 250 m surface. Figure 11d shows the vertical cross section of vector wind and vertical velocity at $y = -110$ km which roughly cuts through the center of the lee mesolow. A stagnation point associated with the flow recirculation forms at about $x = -120$ km near the surface upstream of the mountain on this vertical plane. For a higher-Froude number flow over Taiwan, the disturbance is similar to the present case but with a much more pronounced inertia-gravity wave response.

Table 2. *Summary of Numerical Experiments with the Taiwan Topography*

Case	T1	T2	T3	T4
Fr	0.125	0.125	0.125	0.125
U (ms^{-1})	5	5	5	5
Impinging angle	225° (SW)	270° (W)	270° (W)	45° (NE)
f (s^{-1})	5.8×10^{-5}	5.8×10^{-5}	0	5.8×10^{-5}

4.2 Westerly Flow Past CMR (Case T2)

Figure 12 shows the streamlines, pressure perturbation, and vertical velocity at $z = 250$ m and the vertical cross section at $y = -110$ km for an inviscid stratified flow past the real topography of Taiwan after 10 h. The basic flow is from the west with a speed of $5\,\mathrm{ms}^{-1}$. The Froude number and Coriolis parameter are the same as in case T1. A stagnation point forms upstream of the island and one lee vortex forms to the eastern slope of the CMR. Apparently, this vortex is similar to those found in the idealized simulations (Fig. 2). As in the idealized topography cases, the formation mechanism of this lee mesovortex may be explained by the baroclinically-induced vorticity tilting as

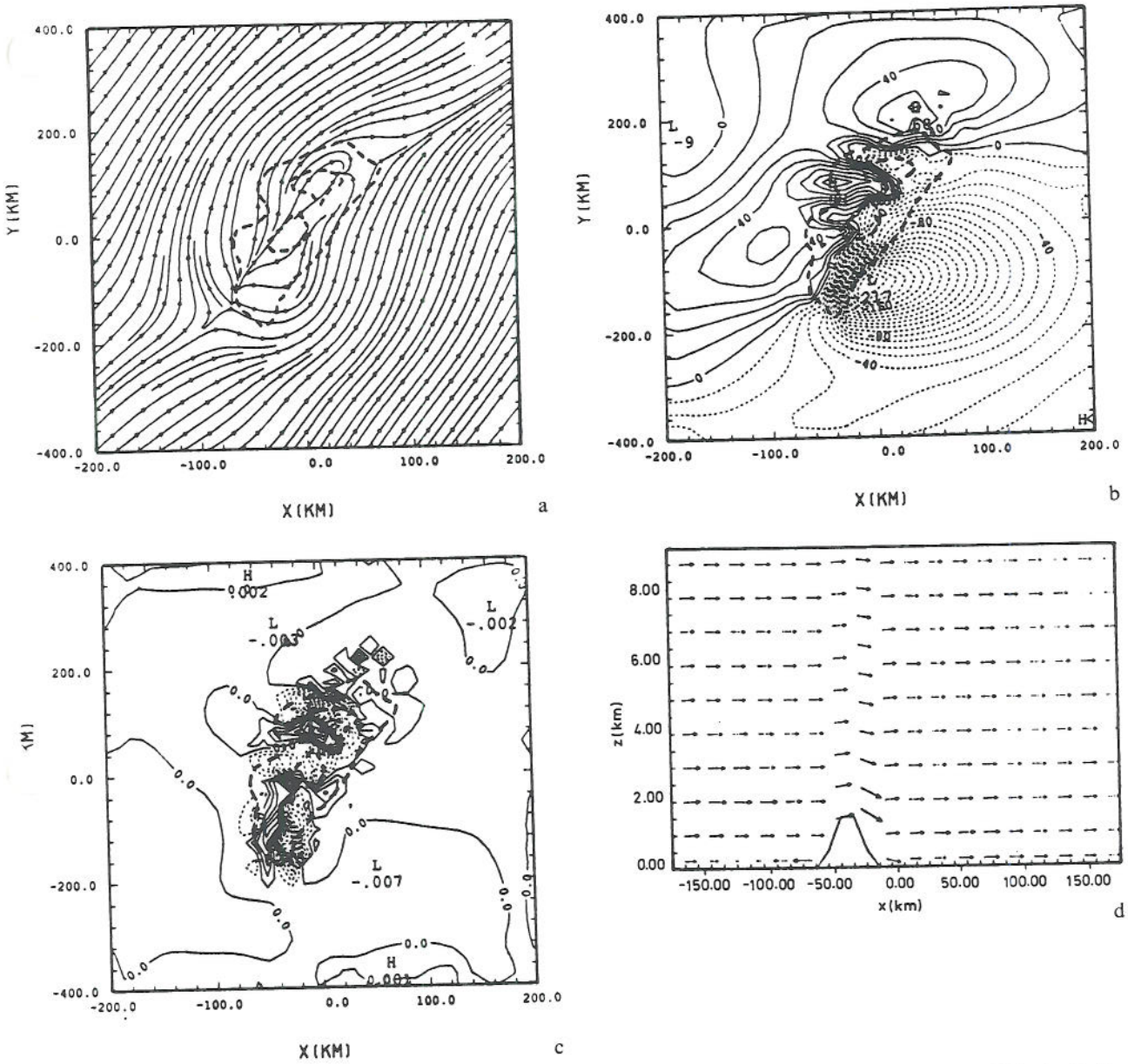

Fig. 11. (case T1) Southwesterly flow over the real topography of Taiwan. The Froude number is about 0.125. The basic flow speed and Brunt-Vaisala frequency are $5\,ms^{-1}$ and $0.01\,s^{-1}$. The Coriolis parameter is $5.8 \times 10^{-5}\,s^{-1}$. Contours of 500 and 2500 m of the mountain height are depicted by heavy dashed curves. Four fields after 10 h are shown: (a) streamlines on 250 m surface, (b) perturbation pressure (Exner function, contours from -0.21 to $0.09\,J\,kg^{-1}\,K^{-1}$), (c) vertical velocity on 250 m surface (contours from -0.22 to $0.14\,ms^{-1}$), and (d) vector wind and vertical velocity on the vertical plane at $y = -110$ km

the gravity waves steepen, overturn, and break. No northeast vortex has been produced at this time, which is weakened by the rotational effects as discussed in the previous section (case I2) and which will be shown later. Similar to case T1, the perturbation pressure field (Fig. 12b) shows a strong pressure gradient across the mountain range. A mesohigh forms to the northwest of the CMR, while a major mesolow forms to the southeast. This mesolow is located about 80 km to the southwest of the lee vortex. Thus, the downslope wind passes through the mesolow center. This response is similar to the flow response past an idealized bell-shaped mountain (cases I1 and I2), in which the mesolow is not collocated with the lee vortices. Again, the upstream mesohigh and the leeside mesolow can be explained by the hydrostatic mountain wave theory.

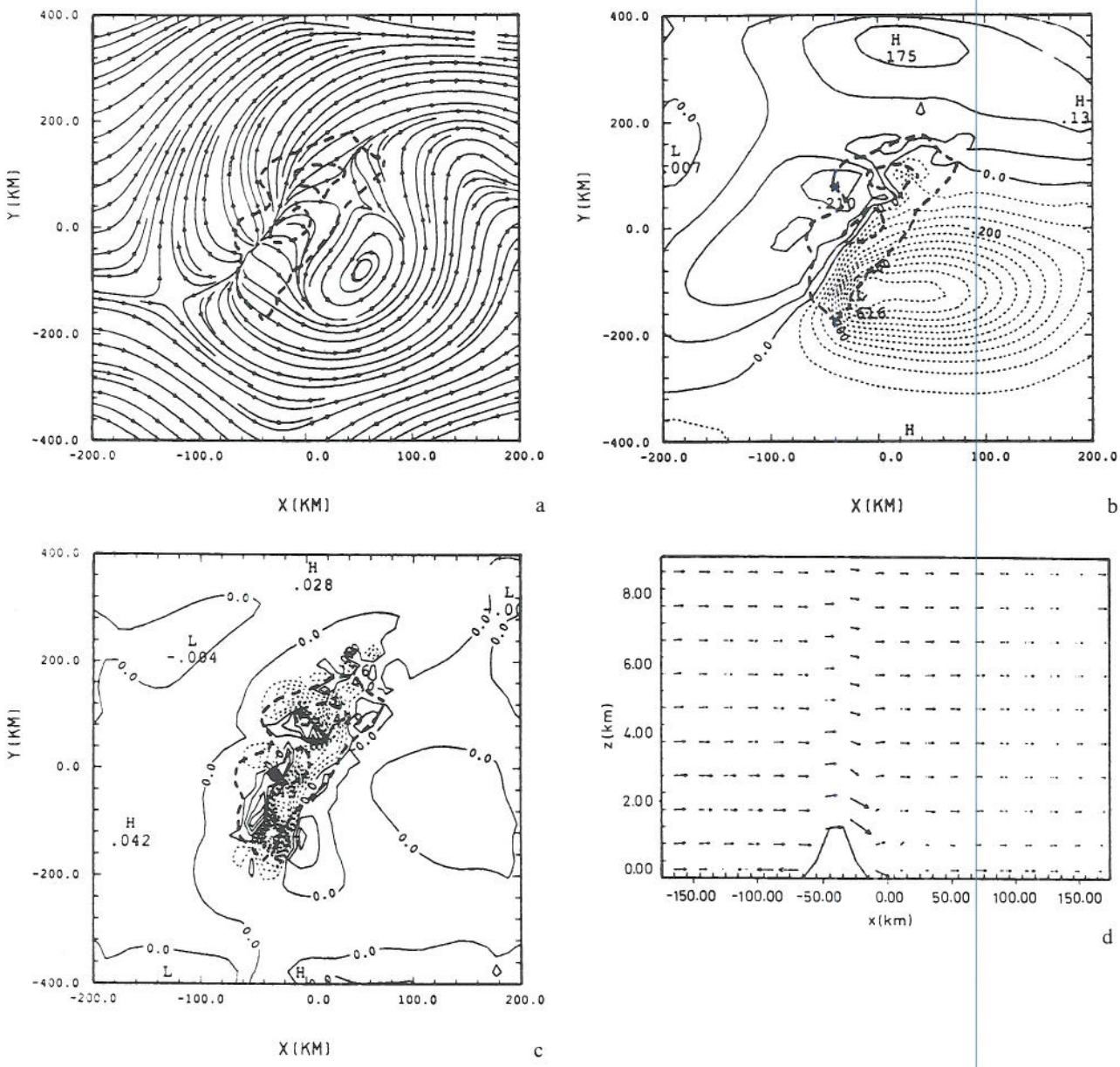

Fig. 12. (case T2) Same as Fig. 11 but with westerly flow. Contours of the pressure perturbation and vertical velocity from -0.6 to $0.2\,\mathrm{J\,kg^{-1}\,K^{-1}}$ and from -0.91 to $0.28\,\mathrm{ms^{-1}}$, respectively

There exist two major regions of upward motion located just upstream of the two CMR peaks (Fig. 12c). Two regions of weak upward motion also form to the northeast and southeast of the CMR, again which are dictated by the flow convergence imposed by the momentum equation (Fig. 12a). Figure 12d shows the vertical cross section of vector wind and vertical velocity at $y = -110\,\mathrm{km}$ which roughly cuts through the center of the lee mesolow. A stagnation point forms at about $x = -125\,\mathrm{km}$ near the surface. On the lee slope, there exists a region of relatively stronger winds. There exists no flow steepening above the mountain peak on this vertical plane. This is because the overall mountain height is lower at this particular location. The relatively stronger downslope wind at this location can strengthen the lee mesolow through the mechanism of adiabatic warming.

Similar to the idealized topography case of Fig. 4 (case I2), the lee vortices generated by the flow past Taiwan are not steady. The streamlines

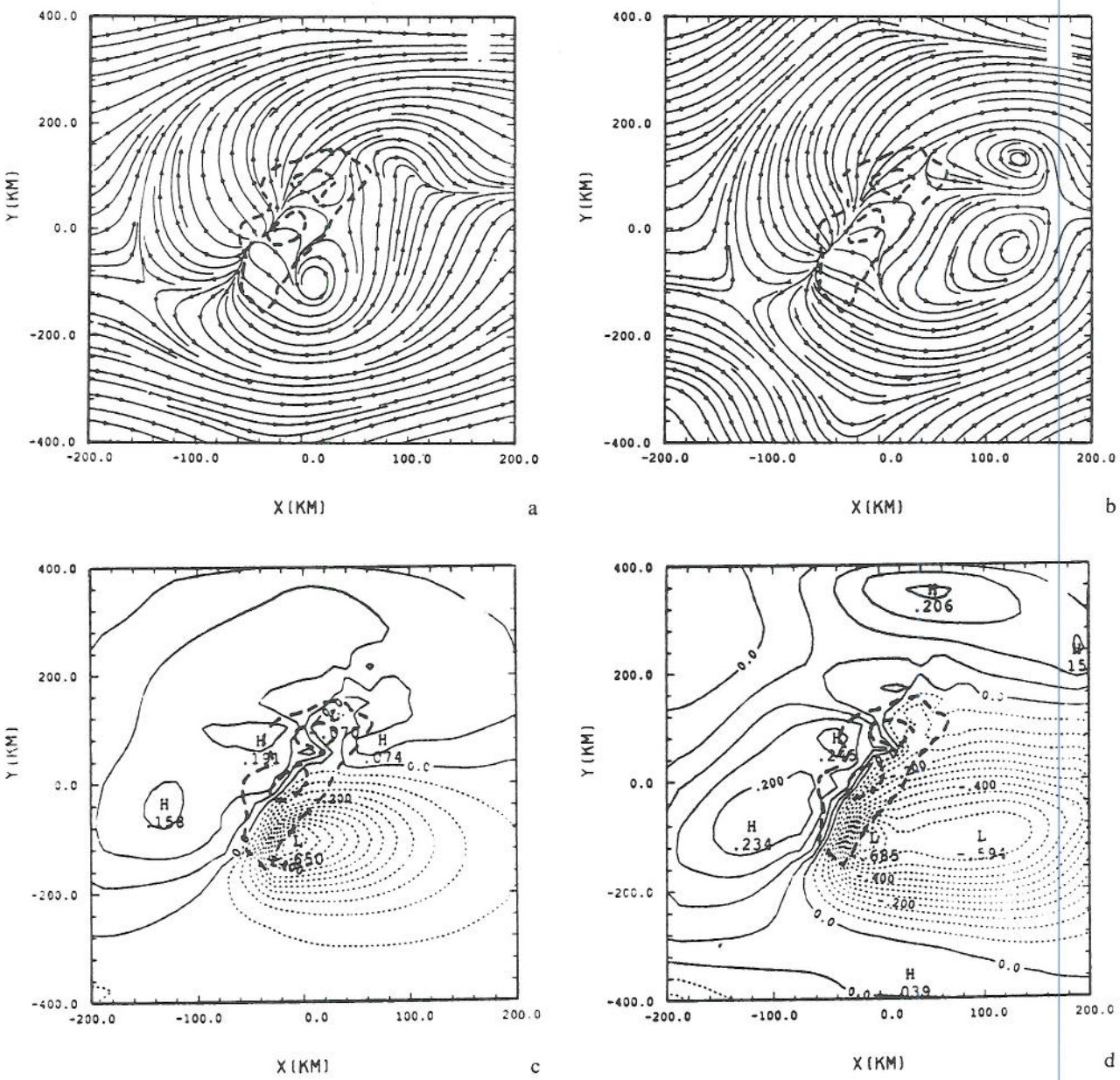

Fig. 13. (case T2) Streamlines for the flow of Fig. 12 after (a) 5 h and (b) 15 h. The corresponding perturbation pressures are shown in (c) and (d)

and perturbation pressure at 5 and 15 h for this case are shown in Fig. 13. At 5 h, a small lee vortex forms to the southeast of the CMR (Fig. 13a). One confluent zone forms to the east of the northern tip of the CMR. The southeast vortex keeps developing and moving northeastward after 10 h (Fig. 12a). At 15 h, a new vortex forms to the north of the existing vortex (Fig. 13b). The circulation associated with the new vortex is anticyclonic. It is anticipated that both vortices will keep moving farther downstream at later times. Similar to case I2 (Fig. 4), the northern vortex forms at a later time than the southern vortex because it takes a longer time for the fluid particle to reach the northern part of the mountain. Notice that the flow near the mountain and the perturbation pressure (not shown) reaches a quasi-steady state after 10 h. This result is similar to the observations of Kuo and Chen (1990) and the numerical simulation of Sun et al. (1991).

At 5 h and 10 h (Figs. 13c and 12b, respectively), there exists only one mesolow to the southeast of

Taiwan, which is formed by the orographically forced downslope wind through adiabatic warming. However, there is a new mesolow which develops by 15 h (Fig. 13d). This mesolow is collocated with the cyclonic mesovortex and moves downstream with it. Similar to the finding in case I2, this combined mesolow and vortex may be regarded as a *mesocyclone*. This mesocyclone may be related to the mesocyclone located to the east of Taiwan as observed in TAMEX by Kuo and Chen (1990, see Figs. 1c and 1d).

4.3 Nonrotating Flow Past CMR (Case T3)

To investigate the rotational effects of an inviscid stratified flow past Taiwan, we simulate a case similar to case T2 which neglects the effects of planetary rotation (Fig. 14). The flow pattern in the vicinity of the island is similar to the rotating case (Fig. 12a). However, there is a significant difference on the lee side. In the present case, there exists a northeast mesoscale lee vortex in addition to the southeast vortex. This result is similar to the finding of case I2. It appears that the Coriolis force tends to strengthen the southeast (cyclonic) lee vortex and weaken the northeast (anticyclonic) lee vortex. This is due to the addition of the positive planetary vorticity associated with the earth's rotation. The perturbation pressure in this case is similar to that of Fig. 12b except with a stronger low pressure center present over the northern part of the downwind slope.

4.4 Northeasterly Flow Past CMR (Case T4)

Figure 15 shows the results after 10 h for a case similar to case T1 except that the basic flow is from the northeast. Similar to the southwesterly flow case, no stagnation point forms upstream and no vortices form on the lee side of the CMR. A perturbation high pressure region forms to the east of Taiwan. A strong pressure gradient develops across the CMR. A pronounced cyclonic circulation forms to the northwest of Taiwan. Associated with this cyclonic circulation is a mesoscale low pressure region with the center located slightly to the southwest of the cyclonic circulation center. This low may be identified as the northwest mesolow observed during the Mei-Yu season. The formation mechanism of this northwest low is similar to that of the westerly and southwesterly cases. The less frequent occurrence of the northwest mesolow may be due to the smaller impinging angle of the prevailing northeasterly or northerly flow behind the Mei-Yu front.

5. Concluding Remarks

In this study, several numerical experiments have been performed for inviscid, continuously strati-

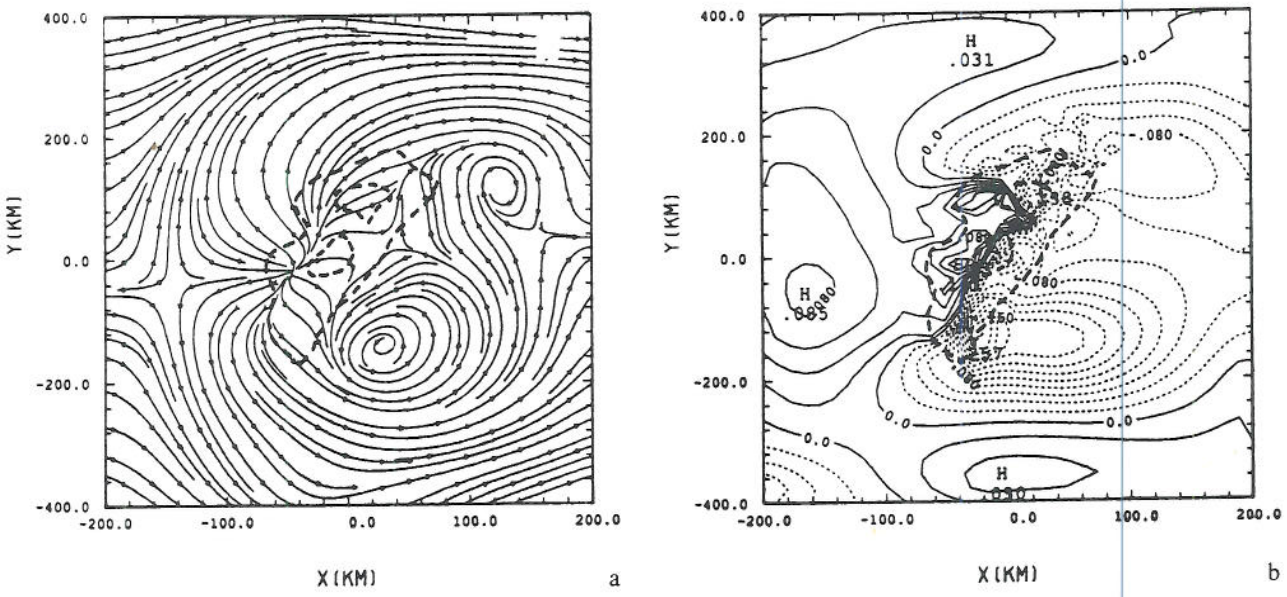

Fig. 14. (case T3) Same as Fig. 12 but without planetary rotation. Only streamlines (a) and perturbation pressures (b) are shown

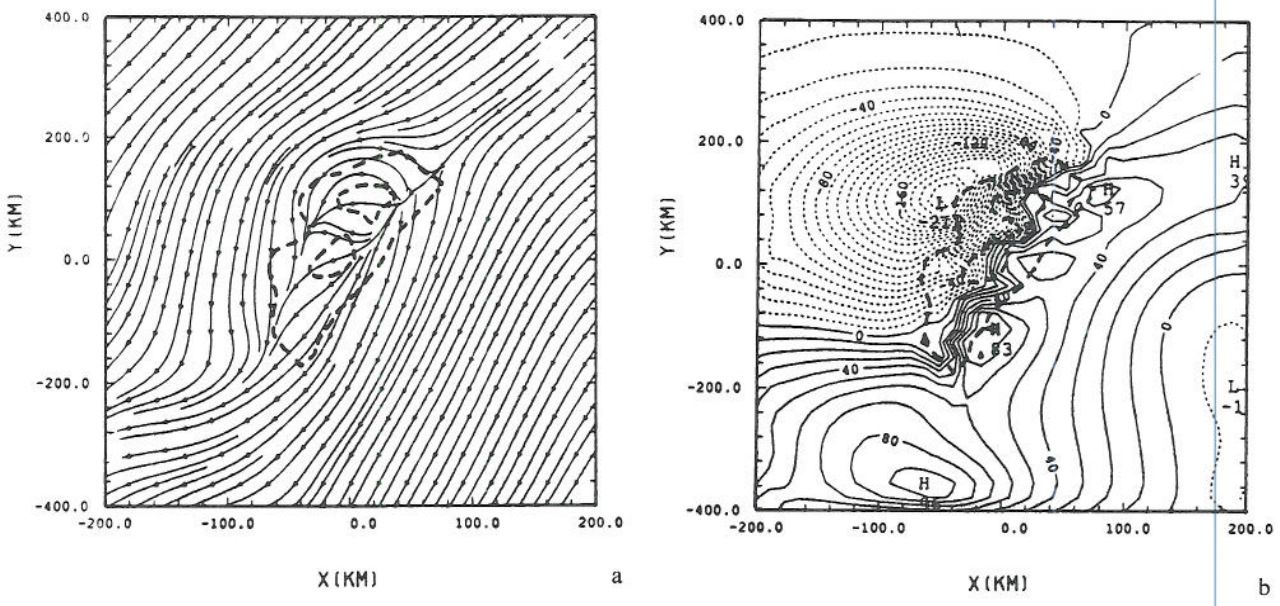

Fig. 15. (case T4) Same as Fig. 11 except for northeasterly flow. Only streamlines and perturbation pressures are shown. Contours of perturbation pressure from -0.21 to $0.09\,\mathrm{J\,kg^{-1}\,K^{-1}}$

fied flow past either an idealized topography or the real topography of Taiwan to investigate the flow response. The formation and development of lee mesolows, mesovortices, and mesocyclones are discussed.

For an inviscid nonrotating flow past a circular bell-shaped mountain with low Froude number, an attachment point and a stagnation point form on the upstream side of the mountain, a region of wave steepening forms above the mountain peak and a pair of cyclonic and anticyclonic vortices form to the lee side. These features are similar to the finding of Smolarkiewicz and Rotunno (1989a). However, it is found that the lee vortices are transient, which move farther downstream and the flow reaches a quasi-steady state near the mountain at later times. The advection speed of the lee vortices is about two-thirds of the basic wind velocity, which is due to a reversed pressure gradient just upstream of the lee vortices. Our results indicate that the formation of the lee vortices takes place progressively. The formation of the lee vortices may be explained by the baroclinically-induced vorticity tilting as the mountain waves become more and more nonlinear. It appears that this formation mechanism is a merger of the theories proposed by Smith (1989b) and Smolarkiewicz and Rotunno (1989a). However, some inconsistencies still exist among the present numerical results and their theories. For example, the lee vortices do not concur with the upslope stagnation point in time as suggested by Smolarkiewicz and Rotunno (1989a) and predicted by the lee eddy theory of Smith (1989b), but rather form at a later time. Our results also indicate that there exists no wave overturning and breaking over the lee slope (Figs. 2, 5, and 8). This is different from that found in Crook et al. (1990). The lack of wave overturning and breaking may be viewed by a separate phenomenon form the lee-vortex formation (Rotunno and Smolarkiewicz, 1991). Further investigations are needed to resolve this problem.

It is found that a pair of lee mesovortices forms for a flow with $Fr = 0.66$, although they take a longer time to form than those associated with lower-Froude number flows. This result is consistent with the prediction of Smith (1989c). Due to the smaller scale of the lee vortices generated for a moderately low Froude number ($0.5 < Fr < 0.75$) flow, a finer grid resolution is needed to resolve the structural details of the mesovortices.

A stationary mesohigh and mesolow pressure couplet forms across the mountain, which is produced in both high and low-Froude number flows. The lee mesolow is formed mainly by the downslope wind associated with mountain waves through adiabatic warming. The results of the high Froude number simulations agree well with

the classical results predicted by linear, hydrostatic mountain wave theory. The lee mesolow does not necessarily collocate with the vortices. No obvious stretching of the air column associated with the lee mesolow is found.

The earth's rotation acts to strengthen (weaken) the cyclonic (anticyclonic) vortex and shifts the lee mesolow to the right for an observer facing downstream. The cyclonic vortex then develops into a mesocyclone at later times. The low pressure associated with this mesocyclone can be explained by the addition of planetary vorticity through the momentum equations. The formation of this mesocyclone may be related to the lee cyclogenesis problem associated with the CMR and the Denver Cyclone (Szoke et al., 1984; Crook et al., 1990).

For flows with the same Froude number and strength of nonlinearity, a steeper mountain tends to produce a stronger disturbance. It is found that the lee vortices do not necessarily form simultaneously with the stagnation point on the upstream slope, but rather form at a later time. For high-Froude number flows ($Fr > 1$), there is no formation of a stagnation point on the upstream slope and no mesovortex on the lee. The flow patterns are consistent with the linear, hydrostatic mountain wave theory.

For a southwesterly flow past Taiwan, there are no stagnation points or lee vortices formed because the impinging angle of the flow is small. A mesolow forms to the southeast slope of the mountain, which may be regarded as the Taiwan mesolow. Similar to flow over idealized topographies, the southeast mesolow is formed by the downslope wind associated with mountain waves through adiabatic warming. It is shifted to the southeast by the earth's rotation. A mesohigh forms upstream of the CMR, which produces a strong pressure gradient across the mountain. For a westerly flow past the real topography of Taiwan, a stagnation point forms upstream of the mountain and a pair of vortices form on the lee and move downstream at later times. The southern lee vortex forms earlier than the northern vortex due to the NNE-SSW orientation of the CMR. The cyclonic vortex then develops into a mesocyclone at later times. For a northeasterly flow past Taiwan, the response is similar to the southwesterly flow case except that the mesolow forms to the northwest of the mountain.

With the present numerical results and the observations of Kuo and Chen (1990, Figs. 1c and d), we may propose a conceptual model as shown in Fig. 16. This conceptual model suggests that a stationary mesohigh forms on the upstream and a mesolow forms on the southeast of the CMR under a prevailing westerly or southwesterly flow. An additional moving mesocyclone develops to the east of the CMR if the impinging angle of the prevailing wind is large.

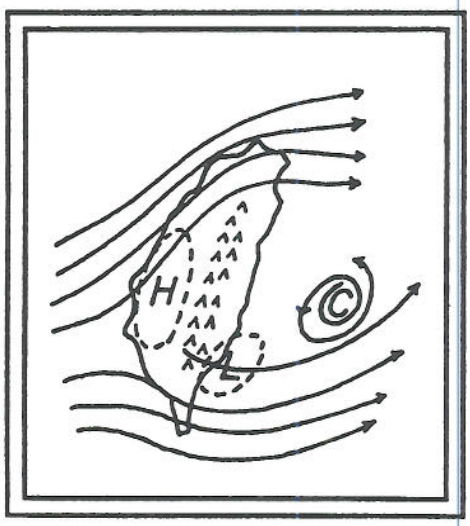

Fig. 16. A conceptual model of the Taiwan southeast mesolow and mesocyclone. A stationary mesohigh forms on the upstream and a mesolow forms on the southeast of the CMR under a prevailing westerly or southwesterly flow. An additional moving mesocyclone develops to the east of the CMR if the impinging angle of the prevailing wind is large

This study suggests that the distinction between the Taiwan mesolow and the lee vortex should be made because they do not necessarily collocate. Thus, more careful data analysis for the Taiwan mesolow is needed. In addition, the formation mechanisms of the lee mesovortices still need to be investigated due to the new finding of the transient features. This transience occurs for both idealized and real topographies. Even though Smolarkiewicz and Rotunno (1989a) stated that the only source of vertical vorticity in their numerical experiments is the baroclinically-induced vorticity tilting, the contribution of the stretching term to the vertical vorticity at later times, such as that found in Sun et al. (1991), may not be ignored once the vertical vorticity has developed from either the potential vorticity generation or baroclinically-induced vorticity tilting. The relative importance of this stretching term and tilting term needs to be investigated. The application of

the lee mesocyclone to the real lee cyclogenesis problem also deserves a further study.

Acknowledgments

Stimulating discussions with R. B. Smith, R. Rotunno, P. K. Smolarkiewicz, W.-Y. Sun, S.-T. Wang, G. S. Janowitz, and M. L. Kaplan are highly appreciated. The authors also wish to thank R. A. Pielke and W. R. Cotton of Colorado State University for allowing the use of their numerical model.

References

Arya, S. P. S., 1988: *Introduction to Micrometeorology*. San Diego: Academic Press, 303 pp.

Batchelor, G. K., 1967: *An Introduction to Fluid Dynamics*. Cambridge, Great Britain: Cambridge University Press, 615 pp.

Chen, G. T.-J., 1980: Mesoscale analysis for a Mei-Yu case over Taiwan. *Pap. Meteor. Res.*, **2**, 63–74.

Crook, N. A., Clark, T. L., Moncrieff, M. W., 1990: The Dever cyclone. Part I: Generation in low Froude number flow. *J. Atmos. Sci.*, **47**, 2725–2742.

Ertel, H., 1942: Ein neuer hydrodynamischer Wirbelsatz. *Meteorol. Z.*, **59**, 271–281.

Huang, C.-Y., Raman, S., 1990: Numerical simulations of Taiwan Island circulations: Boundary layer modification. Workshop on TAMEX Scientific Results, pp 194–198.

Hunt, C. R., Snyder, W. H., 1980: Experiments on stably and neutrally stratified flow over a model three-dimensional hill. *J. Fluid Mech.*, **96**, 671–704.

Klemp, J. B., Durran, D. R., 1983: An upper boundary condition permitting internal gravity wave radiation in numerical mesoscale models. *Mon. Wea. Rev.*, **111**, 430–444.

Kuo, Y.-H., Chen, G. T.-J., 1990: The taiwan area mesoscale experiment (TAMEX): An overview. *Bull. Amer. Meteor. Soc.*, **71**, 488–503.

Orlanski, I., 1976: A simple boundary condition for unbounded hyperbolic flows. *J. Compu. Phys.*, **21**, 251–269.

Queney, P., 1947: Theory of perturbations in stratified currents with applications to airflow over mountain barriers. Dept. of Meteorology, Univ. of Chicago, Misc. Report No. 23.

Rotunno, R., Smolarkiewicz, P. K., 1991: Further results on lee vortices in low-Froude-number flow. *J. Atmos. Sci.*, **48**, 2204–2211.

Smith, R. B., 1980: Linear theory of stratified hydrostatic flow past an isolated mountain. *Tellus*, **32**, 348–364.

Smith, R. B., 1982: Synoptic observations and theory of orographically disturbed wind and pressure. *J. Atmos. Sci.*, **39**, 60–70.

Smith, R. B., 1989a: Hydrostatic airflow over mountains. *Adv. Geophys.*, **31**, 1–41.

Smith, R. B., 1989b: Comment on "Low Froude number flow past three-dimensional obstacles. Part I: Baroclinically generated lee vortices". *J. Atmos. Sci.*, **46**, 3611–3613.

Smith, R. B., 1989c: Mountain induced stagnation points in hydrostatic flows. *Tellus*, **41A**, 270–274.

Smolarkiewicz, P. K., Rasmussen, R., Clark, T. L., 1988: On the dynamics of Hawaiian cloud bands: Island forcing. *J. Atmos. Sci.*, **45**, 1872–1905.

Smolarkiewicz, P. K., Rotunno, R., 1989a: Low Froude number flow past three-dimensional obstacles. Part I: Baroclinically generated lee vortices. *J. Atmos. Sci.*, **46**, 1154–1164.

Smolarkiewicz, P. K., Rotunno, R., 1989b: Reply. *J. Atmos. Sci.*, **46**, 3614–3617.

Smolarkiewicz, P. K., Rotunno, R., 1990: Low Froude number flow past three-dimensional obstacles. Part II: Upwind flow reversal zone. *J. Atmos. Sci.*, **47**, 1498–1511.

Sun, W.-Y., Chern, J. D., Wu, C.-C., Hsu, W.-R., 1991: Numerical simulation of mesoscale circulation in Taiwan and surrounding area. *Mon. Wea. Rev.*, **119**, 2558–2573.

Szoke, E. J., Weisman, M. L., Weisman, Brown, J. M., Caracena, F., Schlatter, T. W., 1984: A subsynoptic analysis of the Denver tornado of 3 June 1981. *Mon. Wea. Rev.*, **112**, 790–808.

TAMEX, 1985: Taiwan Area Mesoscale Experiment: Overview document. NCAR.

Thorsteinsson, S., 1988: Finite amplitude stratified air flow past isolated mountains. *Tellus*, **40A**, 220–236.

Tripoli, G. J., Cotton, W. R., 1982: The Colorado State University three-dimensional cloud/mesoscale model – 1982. Part I: General theoretical framework and sensitivity experiments. *J. de Rech. Atmos.*, **16**, 185–220.

Wang, S.-T., 1989: Observational study of the orographically induced disturbances during TAMEX. Workshop on TAMEX Preliminary Scientific Results, 279–286.

Authors' address: Yuh-Lang Lin, Neng-Huei Lin and R. P. Weglarz, Department of Marine, Earth, and Atmospheric Sciences, North Carolina State University, Raleigh, N.C. 27695-8208, U.S.A.

Errata

Numerical Modeling Studies of Lee Mesolows, Mesovortices, and Mesocyclones with Application to the Formation of Taiwan Mesolows

by Y.-L. Lin, N.-H. Lin, and R. P. Weglarz

The following paragraph should be inserted after "...warming and drying." and before "In addition..." on line 7, column 2 of page 45:

The numerical simulation of Sun et al. (1991) indicated that the mesolow is generated by subsidence warming and that the formation of lee vortices comes mainly from stretching, tilting, and artificial friction.

Errata

Numerical Modeling Studies of Lee Mesolows, Mesovortices, and Mesocyclones with Application to the Formation of Taiwan Mesolows

by Y.-L. Lin, N.-H. Lin, and R. P. Weglarz

The following paragraph should be inserted after "...warming and drying." and before "In addition..." on line 7, column 2 of page 45:

The numerical simulation of Sun et al. (1991) indicated that the mesolow is generated by subsidence warming and that the formation of lee vortices comes mainly from stretching, tilting, and artificial friction.